Computers & Graphics 33 (2009) 521–541

Contents lists available at ScienceDirect

Computers & Graphics

journal homepage: www.elsevier.com/locate/cag

Technical Section

A sketch-based approach to human body modelling

Chen Mao, Sheng Feng Qin *, David Wright

School of Engineering and Design, Brunel University, Uxbridge, Middlesex UB8 3PH, UK

ARTICLE INFO

Article history:
Received 29 May 2007
Received in revised form
27 March 2009
Accepted 27 March 2009

Keywords:
Sketch-based approach
Human body modelling
Creative model-based method
Multi-layered generic model
Morphing

ABSTRACT

In this paper, we present a new approach and a novel interface, Virtual Human Sketcher (VHS), which enables those who can draw, to sketch-out various human body models. Our approach supports freehand drawing input and a "Stick Figure→Fleshing-out→Skin Mapping" modelling pipeline. Following this pipeline, a stick figure is drawn first to illustrate a figure pose, which is automatically reconstructed into 3D through a "Multi-layered Back-Front Ambiguity Clarifier". It is then fleshed-out with freehand body contours. A "Creative Model-based Method" is developed for interpreting the body size, shape, and fat distribution of the sketched figure and transferring it into a 3D human body through graphical comparisons and generic model morphing. The generic model is encapsulated with three distinct layers: skeleton, fat tissue, and skin. It can be transformed sequentially through rigid morphing, fatness morphing, and surface matching to match the 2D figure sketch. The initial resulting 3D body model can be incrementally modified through sketching directly on the 3D model. In addition, this body surface can be mapped onto a series of posed stick figures to be interpolated as a 3D character animation. VHS has been tested by various users on Tablet PC. After minimal training, even a beginner can create plausible human bodies and animate them within minutes.

1. Introduction

Human modelling has involved extensive research for many decades. Nowadays, its applications have penetrated many fields including industry, military, biomedicine, and education. In today's public entertainment, virtual humans play a particularly remarkable role when engaged in 3D games, movies, and multimedia (virtual human presenter). Therefore, investigation of simple and efficient ways for creating 3D human body models, especially geometric models, has been an essential theme in the computer graphics field.

Current virtual human generation methods can be classified into three major categories: creative [1–3], reconstructive [4–8], and interpolated [9–12]. Although these approaches are capable of creating highly realistic human body models with various appearances and motions, they generally require extensive expertise, special equipment (traditional/video camera, 3D body scanner, motion capture system, etc.), professional software, and proficient computer skills. Therefore, without special training, it is difficult for ordinary users such as 2D artists and designers to participate and create their own 3D virtual human models.

Recently, researchers have recognised the intuitiveness and importance of sketching as a design tool for 3D modelling and design. Since Teddy's [13] birth in the late 1990s, many casual sketch style interfaces have been developed to transfer user's 2D freehand drawings into 3D freeform surfaces, such as stuffed toys [13–15], simple clothes [16], and self-occluded objects [17]. However, sketch-based modelling of human body surfaces, which are irregular and complex, has remained an open challenge and has rarely been undertaken in the past. Moreover, current sketching interfaces accept mainly single and clean stroke input and enforce a "part-by-part" drawing routine, where one sketch stroke often specifies the shape of an entire object part and users have to complete one part before modelling another. This process conflicts with a "layer-by-layer" drawing routine [18–20], where artists usually first draw "major dynamic lines" followed by profile lines to illustrate an overall object shape. Then, these initial profiles are fleshed-out progressively with suggestive contours and shading/shadow to convey detailed surface features.

In this paper, we present a new approach, which has been implemented into Virtual Human Sketcher (VHS), a prototype system with a sketching interface, enabling anyone who can draw to "sketch-out" 3D human bodies of various body sizes, shapes, and postures. We devised a "Stick Figure→Fleshing-out→Skin Modification" graphical pipeline, inspired by an artistic "layer-by-layer" drawing process. VHS allows freehand sketch input including multiple/overlapping strokes, foreshortening, occlusion, and drawing imperfections. Fig. 1 illustrates the graphical pipeline of this sketch-based human modelling approach and interface.

* Corresponding author. Tel.: +44 1895266335; fax: +44 1895269763.
E-mail addresses: Chen.Mao@acm.org (C. Mao), Sheng.Feng.Qin@brunel.ac.uk (S.F. Qin), David.Wright@brunel.ac.uk (D. Wright).

0097-8493/$ - see front matter © 2009 Elsevier Ltd. All rights reserved.
doi:10.1016/j.cag.2009.03.028

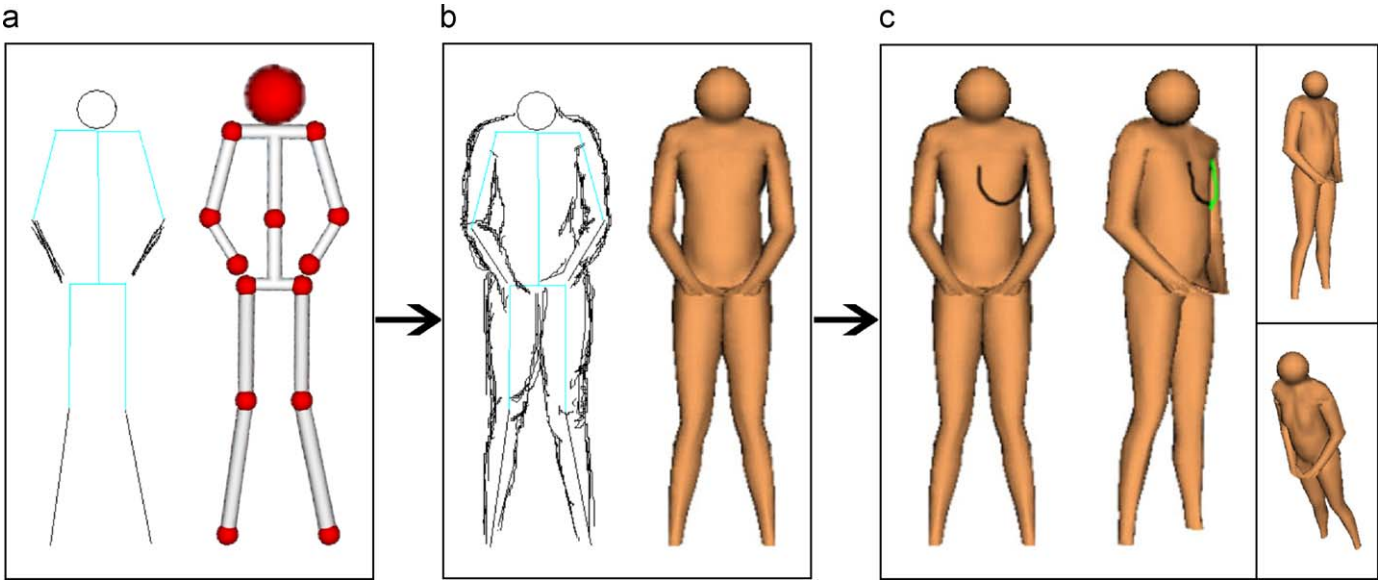

Fig. 1. Sketch-based human body modelling and modification pipeline.

The user first draws a stick figure with depth cues to illustrate a figure pose (Fig. 1a, left). The proposed 3D pose reconstruction method automatically infers the intended pose and reconstructs it into 3D (Fig. 1a, right). The user then fleshes out the initial stick figure with freehand body contours in any sequence as drawing with pencil and paper (Fig. 1b, left). The proposed 3D body modelling approach interprets the body physiques and shape (body profile and fat distribution) from the sketched figure and transfers it into a plausible 3D human surface model (Fig. 1b, right). The user can then incrementally modify this 3D model through over-sketching its 2D contours. Alternatively, the user can rotate the 3D model, view it from different directions, and modify it through drawing a suggestive contour and a view-dependent silhouette contour directly onto the 3D body surface to depict local skin features (Fig. 1c). Once a single body surface is obtained, it can be mapped onto a series of posed stick figures, which can be further interpolated as a 3D character animation [21].

We developed a "Multi-Layered Back-Front Ambiguity Clarifier" [22] for 2D–3D pose recovery from stick figure drawings and an "On-line Stroke Processing Method" for parsing a "noisy" figure flesh-out. Furthermore, we investigated a "Creative Model-based Method", which interprets the body physiques and shape from a 2D contour sketch and transfers it into a 3D human body through graphical comparisons and generic model morphing. Created from Visible Human cross-section images, our generic model is encapsulated with three distinct layers: skeleton, fat tissue, and skin for undertaking both geometric and physical morphing. To handle drawing imperfections, our system VHS provides figure pose auto-correction and shape auto-beautification routines. The initial body shape can be incrementally modified on 2D sketch or on 3D model directly.

The structure of this paper is as follows. Section 2 summarises the previous work in related areas. Section 3 briefs our 3D pose reconstruction method. Section 4 introduces the proposed approach for sketch-based 3D human body modelling. Sections 5, 6, and 7 present detailed techniques on multi-layered generic model acquisition and specification, reconstruction from 2D raw sketches into 3D human body models, and sketch-based local skin surface deformation, respectively. Section 8 discusses the current 3D human body modelling/animation results and a comparison study between VHS and other modelling systems. Section 9 briefs the user evaluation and experiences on VHS. Section 10 presents the limitations and future work of the current approach, before the final conclusions are drawn in Section 11.

2. Related work

Human body modelling is an essential theme of modern computer graphics. Current methodologies in this area can be classified into three major categories: creative, reconstructive, and interpolated. The *creative* approach generally involves creating and interactively designing animatable human bodies without resorting to existing shapes. It includes modelling and animating through current commercial packages (e.g. 3D Studio Max, Maya), and some early anatomically based modellers [1,2], which consist of multi-layers for simulating individual muscles, bones and tissues. While allowing for interactive design, considerable user intervention is required, which results in a relatively slow production rate and a lack of efficient control facilities [23]. The *reconstructive* approach generally builds the 3D body geometry automatically from existing shapes captured by traditional cameras [6,7], video cameras [5], 3D scanners [8], and motion capture systems. Although fast and effective, these body-cloning techniques are limited in generating individualised models, whose shapes can hardly be modified. Lastly, *interpolated* modelling utilises a range of scanned/captured examples to generate new animatable human bodies [9–12] through interpolating the existing ones. In addition, many *reconstructive* and *interpolated* modelling approaches can be identified as "model-based" methods, which employ a morphable generic model and deform it against the captured features [6,7,11], anthropometrical measurements [12,24], linear data interpolation [10], etc. to generate various human bodies or faces.

Sketch-based 3D freeform object modelling has become feasible, as demonstrated by the work of Igarashi et al. [13], Karpenko et al. [14], Tai et al. [25], and Schmidt et al. [26]. In these systems, users draw 2D freeform strokes interactively specifying the silhouette of an object, which is automatically constructed as a 3D freeform surface model represented as polygonal meshes [13], variational implicit surfaces [14], spherical implicit surfaces [15], convolutional surfaces [25], etc. The initial objects can be assembled and refined into final complicated ones by a set of editing operations, such as extrusion, cutting, blob merging,

transformation, etc. in a "part-by-part" manner. The resulting 3D models are mostly smooth, stuffed, and lack of local surface details. Meanwhile, modelling an object is more like assembling a handcraft toy with gestures rather than natural freehand sketching. Since the human body has an irregular and complex surface and our eyes are especially sensitive to its rendering flaws [27], the above modelling approaches constrained by their underlying construction schemes and application context, are not suitable for sketching out plausible virtual humans.

Sketch-based surface deformation has been studied recently. Nealen et al. [28] employed the Laplacian framework in a sketch-based interface for detail-preserving mesh editing. This interface enables sketching of significant surface features on existing shapes through silhouette sketching, feature/contour sketching, and suggestive contour sketching. The deformation region of interest (ROI) is manually selected by users.

In our research, we developed a sketch-based approach to human body modelling, and delivered a fast and easy solution for producing a plausible 3D human body model and its modification through 2D sketching. Inspired by the figure drawing guidelines from many sketch books [18,20], we devised a "Stick Figure→Fleshing-out→Skin mapping" modelling pipeline. This modelling pipeline echoes the modelling and animation pipeline in commercial packages such as 3DS MAX. Users can choose to build simple stick figures, create delicate surface models, or explore further to animate these sketch-generated creatures. 3D models can be exported from VHS to commercial packages (e.g. 3DS MAX, Maya) at any level to be refined by their function kits. More details in this application area are discussed in Section 8.2.

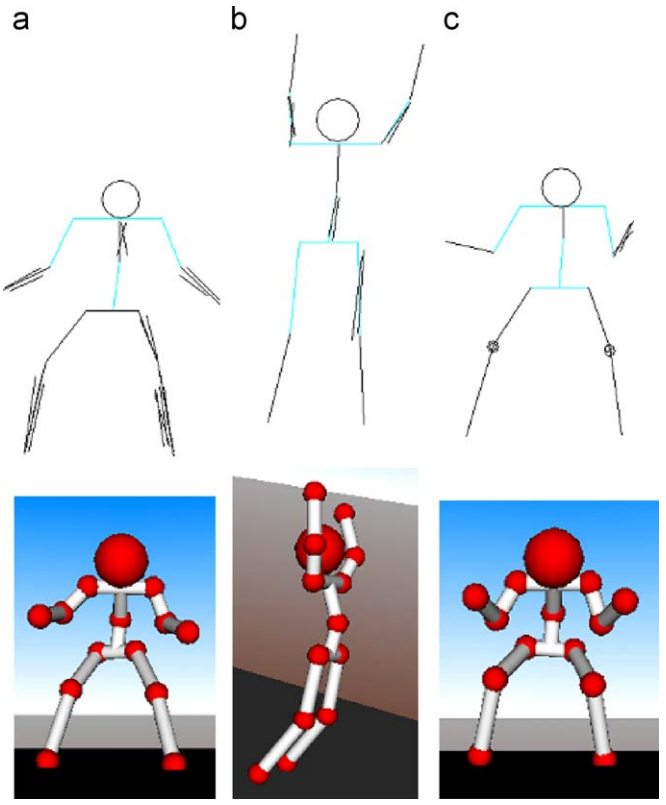

Fig. 2. 2D skeleton drawing and 3D pose recovery: (a) reconstructed 3D poses with thickness rendering gestures. (b) When thickness contrast is not provided, joint ROM is utilised for pose recovery. The left lower leg is identified as bending backwards since bending forwards is against the ROM for a knee joint. (c) The upper torso and left lower arm are similarly posed by employing joint ROM constraints.

3. 3D pose reconstruction from 2D stick figure drawing

According to our human modelling pipeline, the user firstly draws a stick figure to illustrate the body proportion and posture. Given a 2D hand-drawn stick figure under an orthographic view, there is a challenge to reconstruct a unique 3D pose from a set of candidates because of the "back-front ambiguities" problem (each foreshortened bone segment may point either towards or away from the viewer with respect to the image plane). We developed a "Multi-layered Back-front Ambiguity Clarifier" [22], which utilises figure perspective rendering gestures, human joint range of motion (ROM), and key frame coherence to clarify the orientations of foreshortened bone segments layer-by-layer gradually until a unique figure pose is achieved. We integrate the figure perspective rendering technique [18] into the system design and generalise a set of thickness-rendering gestures, which is easy to use and efficient for pose inference by the system. In essence, we arrange bones and joints into different groups and correlate thickness contrast features to depth relationships. Generally, the thicker bone/joint is the closer (see Fig. 2). Compared with other related approaches [29–32], our method features better utilisation of sketch information to assist 3D pose identification. Since perspective rendering is more likely to be used in full figure drawing than stick figure drawing, users can alternatively indicate thickness contrasts while fleshing-out a figure. The system provides on-line drawing assistance to help users maintain correct figure proportion and foreshortening. Moreover, an "overall pose checking/auto-correction" routine is offered to ensure physically valid poses during a quick and imprecise drawing process.

4. Creative model-based 3D body generation scheme

Transferring a single freehand figure sketch into a plausible 3D human body model is mathematically indeterminate because of imprecise and insufficient information. In contrast, humans are accustomed to perceiving 3D objects from sketched geometries based on 2D and 3D correlations [33]. In terms of the perception of raw figure drawings, the human brain can envision their 3D counterparts easily and even spontaneously. Therefore, referring to this perception process may help to formulate the mechanism for automatic 2D-to-3D reconstruction by computers.

Since we see and interact with people every day, our brain is familiar with various body shapes and the correlations between 2D flat features and their real-3D counterparts. In other words, the underlying human body contexts in our mind help to evaluate body geometric and physical elements from a 2D figure drawing and to form its counterpart body reflecting the perceived features. For instance, when we view the drawings of large-sized or muscular figures, our brain can perceive and envision body models of not merely geometric shapes that match the 2D drawings, but also contextual physical attributes such as rounded/over-weighted or firm/muscular features, which reflect the inner body (fat, muscles) composition. Gathering the aforementioned hints and elements, it seems to be feasible to establish a computerised mechanism for 3D body modelling from 2D figure sketches. Given a range of morphable template bodies containing multiple physical layers (i.e. fat, muscles, and skin) as pre-stored body contexts, a computer can interpret the geometric and physical attributes of a figure sketch, and then morph and fit a multi-layered template into the 2D drawing to obtain a matching 3D model.

In terms of the 3D body templates, the statistically parameterised 2-layered (skeleton–skin) models generated from

[10–12] may provide a rich resource of realistic human body shapes. However, each figure sketch depicts an imaginative character, which has a unique and even unrealistic body shape that often blends the features of many different bodies together with its individualised attributes. Thus, it is very hard to find a matching model from existing body geometries, through a fixed number of sizing parameters [10–12]. Since human brains can envision and are aware of the physical attributes (i.e. fatness, muscularity) of figure sketches, which are affected by body inner structures, it is arguably necessary to introduce more inner body layers (i.e. fat, muscles, etc.) into the current two-layered (skeleton–skin) digital templates [10–12]. In fact, a human body is effectively a multi-layered object and the variations of inner body layers often transform the look and shape of the outer body noticeably. In the sense of sketch-based human body modelling, a template model containing more inner layers may imply more inner body contexts for evaluating the physical attributes conveyed in figure sketches, and more flexibility as well as control parameters to match an existing template into a 2D figure sketch through both geometric and physical morphing. In our current approach, we adopted a three-layered (skeleton–fat tissue–skin) anatomical model, because compared with muscles, the fat is more variable and dominant in affecting the overall body shape.

Inspired by the hints and elements of human perception, we devised a "Creative Model-based Method", which can process a rough figure sketch, interpret its body size (skeleton proportion) and shape (body profiles and fat distribution), and transfer it into a plausible 3D counterpart model through graphical comparisons and generic model morphing (rigid morphing, fatness morphing, and surface matching, see Fig. 3). Here, an orthographic projection is utilised to project the silhouette of the 3D generic model to 2D for comparisons with the original 2D figure sketch. Our 3-layered generic model is digitised from the anatomical male cross-section images of The Visible Human Project® [34]. A whole body fat distribution map has been digitised comprising the fat accumulation conditions (fat percentage value) of each individual body part, each sample cross-section, and each sample skin point.

Based on our "Stick Figure→Fleshing-out" drawing routine, each sketch-generated model is readily animatable. It inherits the skin-binding conditions of the 3D generic model. Our current system cannot support sketch-based modelling of human head/hands/feet, which is also a common challenge for other related approaches.

According to the aforementioned 3D body generation scheme, following research questions are to be addressed: (1) How to generate a 3-layered generic model and make it geometrically and physically morphable? (2) How to process a "noisy" figure sketch with multiple/overlapping strokes, missing body contours, and drawing imperfections? (3) How to deduce the body features from a sketched figure and transfer it into a plausible 3D body model through continuous graphical comparisons and generic model morphing? (4) How to enable global and local skin surface modifications through 2D sketching?

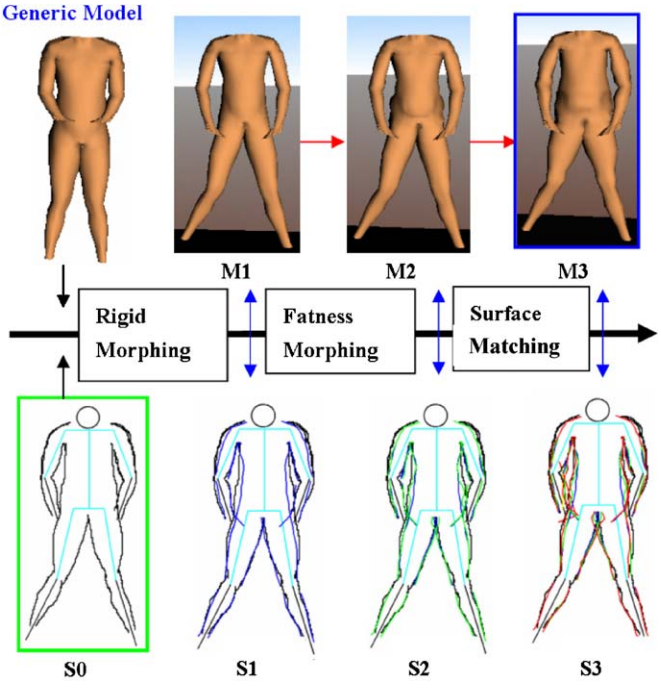

Fig. 3. Transfer a 2D freehand sketch into a 3D body model through an automatic system recognition and morphing process: Users draw a 2D figure (S0). The system automatically retrieves its 3D pose and body proportion, and performs a rigid morphing on the 3D generic model. The resulting 3D model M1 is projected into 2D (blue lines in S1) and compared with the original sketch (black lines) to evaluate its body fat distribution. M1 is then deformed through fatness morphing into M2, which is projected (green lines in S2) and compared again with the 2D sketch to get the matching measurements. The final 3D model (M3) is delivered to users, after an automatic surface matching and beautification process (on M2). Users can incrementally refine their 2D sketches; a similar process is performed to produce the updated 3D model. Here, after fatness morphing, the body lower torso is "fattened" resulting in a changed overall shape with effects of a stuffed and overweighted belly, which can hardly be achieved by pure geometric scaling of the template model.

5. Generic model acquisition and specification

The 3-layered generic model in our system is reconstructed from the cadaveric cross-section images from the Visible Human Project® (VHP), since they exhibit a precise relationship between the skeleton, fat tissue, and skin. The preparation of this multi-layered anatomical model consists of the following five procedures: (1) Virtual skeleton registration, (2) Skin mesh recovery, (3) Template fat distribution digitisation, (4) Body-fattening scheme specification, and (5) Skin binding.

5.1. Virtual skeleton registration

In the early version of this system [22], a simplified skeleton model was adopted. It contains 12 bone segments and 13 joints (see Fig. 4a). All bones are hierarchically linked. The body root is the mid-point of the lower torso. In our current system, this plain representation is maintained since it is easy to draw and expedient for system pose recovery. To apply this simple skeleton to a real human body, we used a semi-automatic image registration method (Illustrated in Fig. 5). After skeleton adaptation, the information of 3D joint coordinates and 2D bone lengths are extracted from the original anatomical model. Then, these measurements are further normalised to achieve a template skeleton, which conforms to the scale and global origin (body root) of the system's pre-stored reference skeleton.

5.2. Skin mesh reconstruction

To digitise the skin mesh, we divide the overall body into individual parts (e.g. left/right arm, torso, etc.) and perform "ray casting" (see Fig. 4d) for each body part on their indexed and calibrated cross-section images. The ray centres here are acquired from both existing template joints and linear interpolation of the neighbouring joints to obtain the corresponding in-between ray

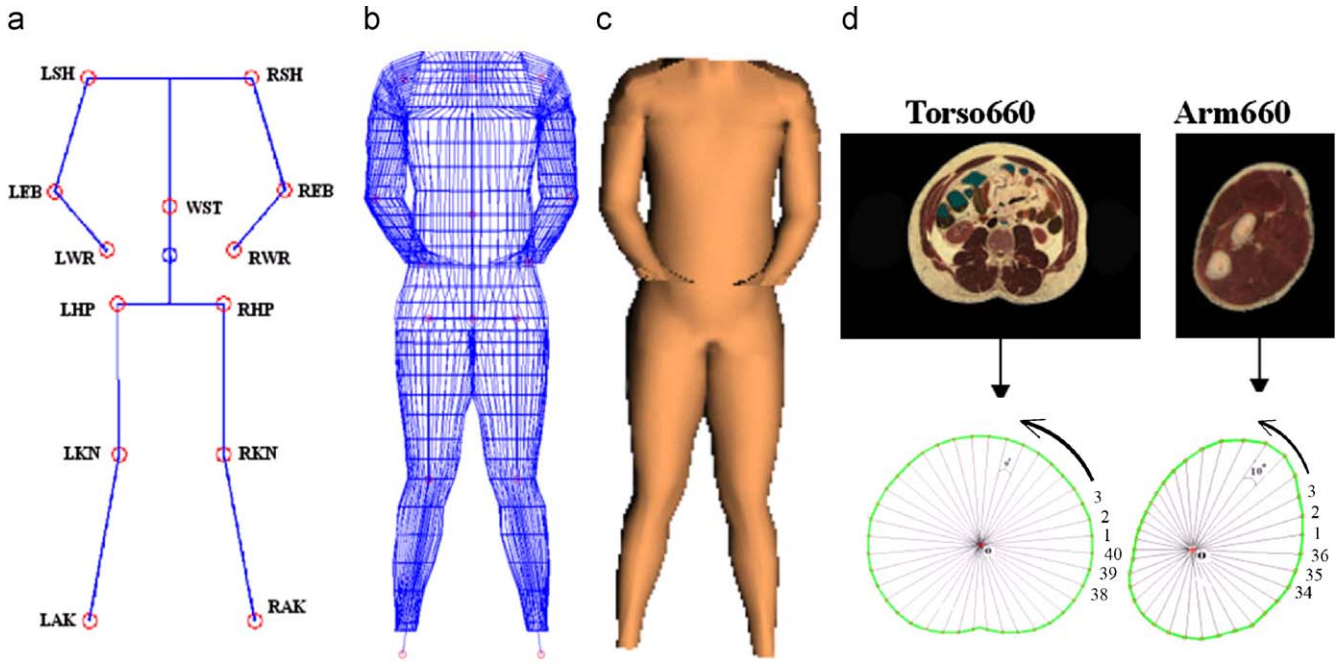

Fig. 4. (a) The template skeleton (joint—red circle, body root—blue circle). (b) The wireframe 3D generic model. (c) The rendered 3D generic model (d) Ray casting the cross-section images for each body part (torso—40 rays, limbs—36 rays) to digitise the 3D template from the human cadaveric images. The ray centre O is the estimated sectional bone position. The image index indicates the corresponding body part and the distance from the head top to the given cross-section slice. (For interpretation of the references to colour in this figure legend, the reader is referred to the web version of this article.)

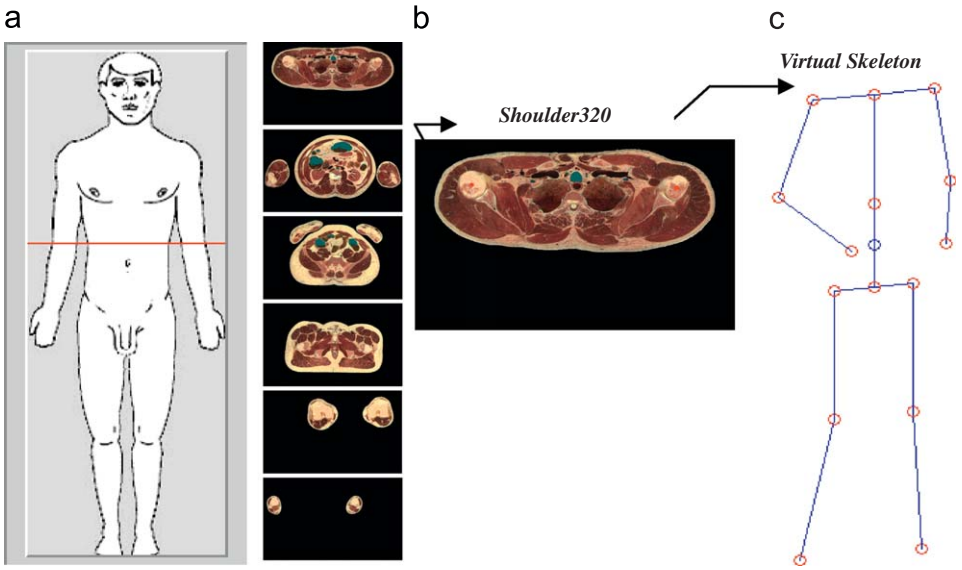

Fig. 5. Virtual skeleton reconstruction: (a) the cross-section images containing the estimated key body joints. (b) Marking the estimated joint positions, and retrieving their 2D locations (*X*/*Y* coordinates) through image processing. (c) The reconstructed and normalised 3D virtual human.

centres. Then, the boundary casting points (surface points) on each body cross-section are indexed and transformed from the local system (centred at the sectional ray centre) to the global system (centred at the body root). The 3D template model is constructed by connecting all these 3D casting points horizontally and vertically, which results in a wireframe model with 3136 mesh vertices (see Fig. 4b). This ray casting generated model has an inherent quad-patch grid structure, which enables easy feature extracting from the raw figure sketches and piecewise affine transformation of the 3D template (detailed in Section 6).

5.3. Template fat distribution digitisation

Instead of a general fat distribution [12] describing typical body shapes (e.g. apple, pear, etc.), we developed a comprehensive distribution map, which comprises the fat-accumulating conditions for each body part, each sample cross-section, and approximately each sample skin point. Fig. 6 illustrates how the body fat distribution is digitised from anatomical cross-section images.

First, "ray casting" is performed for each pair of cross-section images (with and without the fat layer). Then, given the ray centre

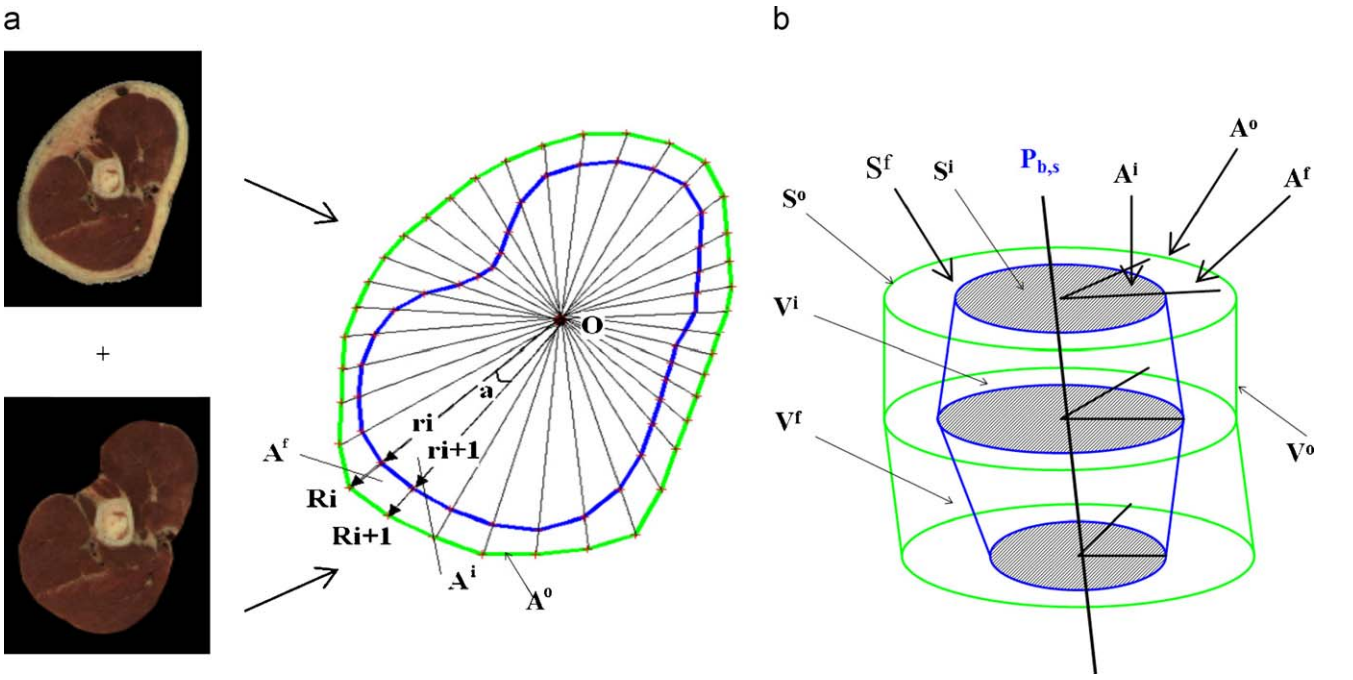

Fig. 6. (a) Ray casting each pair of cross-section images (with and without fat layer) to retrieve the inner and outer radii for each sectional ray. (b) Digitising the template fat distribution.

coordinates, the inner and outer ray radii (r_i and R_i) are computed for each casted ray. Since each cross-section has been evenly distributed into small angular slices (see Fig. 6a), the area for each inner slice (inside the fat layer) and overall slice (fat layer+inner layer) can be calculated by Eqs. (1) and (2):

$$A_i^i = \frac{(r_i\, r_{i+1})}{2}\sin(\alpha) \tag{1}$$

$$A_i^o = \frac{(R_i \times R_{i+1})}{2}\sin(\alpha) \tag{2}$$

($\alpha = 10^\circ$ for limbs and $\alpha = 9^\circ$ for torso), which can be further accumulated to achieve the cross-sectional inner and overall area through integral Eqs. (3) and (4):

$$S^i = \sum_{i=1}^{m} A_i^i \tag{3}$$

$$S^o = \sum_{i=1}^{m} A_i^o \tag{4}$$

Here m is equal to the number of casting rays on each cross-section (40 for torso and 36 for limbs). As in Fig. 6b, given the vertical distances in-between each pair of cross-sections, the inner and overall volume (V^i and V^o) of each body part is calculated. The angular/sectional fat area (A_i^f and S^f) and fat volume (V^f) are obtained by subtracting the corresponding inner value from the overall value.

Next, to digitise the template fat distribution, ratio

$$P_b = V^f/V^o \tag{5}$$

and

$$P_{b,s} = S^f/S^o \tag{6}$$

are used first to compute the fat percentages for each body part (P_b) and its n sample cross-sections ($P_{b,1}, \ldots, P_{b,n}$). The sectional fat distribution features are then encoded as:

$$D_{b,s} = P_{b,s}/P_b \quad (s = 1, 2, \ldots, n) \tag{7}$$

Given the sectional fat area (S^f) and angular fat area ($A_1^f, \ldots, A_m^f$), the angular fat distribution is encoded as

$$D_i^a = A_i^f/S^f \quad (i = 1, 2, \ldots, m) \tag{8}$$

Here, *template fat distribution* is used to represent the sectional and angular fatness conditions ($D_{b,s}$ and D_i^a) inside each template body part. Meanwhile, a general *body fat distribution* stands for the varied body part fat percentages across a body.

The body part fat percentage calculation here assumes that the fat locates near the skin in each cross-section and each body part (i.e. upper/lower limbs, upper/lower torso) generally has a cylindrical topology. In the future, this method can be improved through considering that the fat is not always near the skin in some body areas and slight topological changes of some body parts.

5.4. Template fat percentage manipulation

On the completion of *template fat distribution* digitisation, we investigated a *body-fattening scheme*, through which the 3D generic model can be "physically" morphed when given a set of new fat percentage values of individual body parts. These new body part fat percentages are deduced from a user's figure sketch (see Section 6.3). In reality, everyone has a specific body fat distribution pattern, which is generally preserved when a body fattens or slims. According to this, we assume that the fat is distributed according to the original *template fat distribution* ($D_{b,s}$ and D_i^a unchanged), whilst the inner body stays relatively invariable (S^i and A_i^i unchanged). In brief, the area with more fat is more likely to accumulate new fat, and vice versa. Thus, given a new body part fat percentage P_b, the new sectional fat percentages $P_{b,s}$ ($s = 1,2, \ldots, n$) and angular fat areas A_i^f ($i = 1,2, \ldots, m$) can be calculated. Then, preserving the inner radii (r_i) value, the corresponding skin vertex positions can be updated when outer radii (R_i) change.

In more detail, as illustrated in Fig. 6, given a new body part fat percentage P_b, the new sectional fat percentages $P_{b,s}$ ($s = 1,2, \ldots, n$) can be computed through Eq. (5). Then, presuming the sectional

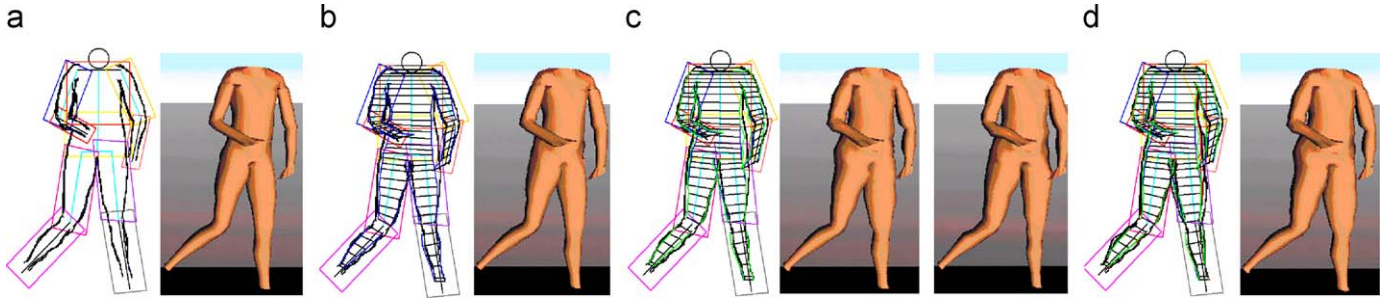

Fig. 7. (a) The input 2D freehand sketch and the 3D model after rigid morphing. (b) Graphical comparison to get the fat distribution measurements and the fatness morphed model. (c) Graphical comparison to get the surface matching measurements; the model with and without auto-beautification. (d) Overtracing body contour (right lower torso, left lower leg, and right leg) to modify an existing 3D surface model.

inner area S_i^i $(i = 1,2,\ldots,m)$ unchanged, the new sectional fat area S_i^f $(i = 1,2,\ldots,m)$ can be calculated. Next, given the preserved $D_i{}^a$ value, the new angular fat area A_i^f on each cross-section can be calculated through Eq. (8). Then, given the Eq. (9),

$$A_i^f = A_i^o - A_i^i\left(\frac{R_i R_{i+1}}{2}\right)\sin(\alpha) - \left(\frac{r_i r_{i+1}}{2}\right)\sin(\alpha) \tag{9}$$

($\alpha = 10^\circ$ for limbs and $\alpha = 9^\circ$ for torso) and preserving the inner radii r_i of each ray, the outer radii R_i can be calculated through solving a equation group:

$$\begin{cases} R_1 R_2 = r_1 r_2 + A_1^f(2/\sin(\alpha)); \\ R_2 R_3 = r_2 r_3 + A_2^f(2/\sin(\alpha)); \\ \vdots \\ R_{n-1} R_n = r_{n-1} r_n + A_{n-1}^f(2/\sin(\alpha)); \\ R_n R_1 = r_n r_1 + A_n^f(2/\sin(\alpha)) \end{cases} \tag{10}$$

($\alpha = 10^\circ$ for limbs and $\alpha = 9^\circ$ for torso). Once the new outer radius of each ray is obtained, its corresponding skin vertex position can be updated, given the original skin vertex position and its original outer ray radius. At this point, all three layers of the generic model have been constructed, and the model is ready for template morphing.

5.5. Skin binding

In the multi-layered generic model, the skin is bound to the underlying skeleton through assigning the affecting bones and corresponding weights for each mesh vertex. A skeleton-driven skin deformation [35] technique is adopted to morph the generic model skin against the new body proportion and posture of a sketched figure during a rigid morphing process. As mentioned earlier, each sketch-created model inherits this skin-to-bone attachment when a "Stick Figure→Fleshing-out" routine is followed.

6. Transfer a 2D raw figure sketch into a 3D human body model

In this section, we introduce the technical details of transferring a 2D raw figure sketch into a 3D human body model through sketch processing and body feature extraction, generic model morphing (rigid morphing, fatness morphing, and surface matching), figure auto-beautification, and incremental 3D model modification by contour over-sketching (see Fig. 7).

6.1. On-line curve stroke processing

Freehand figure sketching is essentially rough and imprecise. It contains various "noises": wiggly/overlapping strokes, missing figure contours, asymmetrical body parts, as shown in Fig. 7a. We devised an "On-line Stroke Processing Method" (see Fig. 8), through which each rendering stroke can be processed instantly to identify its locating bone and saved for body feature extraction. The bone/joint locations on the interface are retrieved when the user draws the initial stick figure. Here, a bounding box is defined for each sketched body part (see Fig. 7a). The default bounding box sizes are determined heuristically based on the generic model proportion and a general body physique. Users can interactively adjust the bounding box sizes (e.g. when drawing a large human) and choose to show or hide the bounding boxes according to their needs. In this on-line sketching system, once a new stroke is applied, the system automatically searches through the entire body to identify which bone the stroke has been fleshing-out, that is, which bone has a bounding box that contains all the curve points of a given stroke. Then, this curve stroke is labelled (according to its assigned bone) and saved for later feature extraction use. Here, confusion may arise when a single stroke is inside the overlapping areas of several body parts, or a stroke is relatively long and spans more than one bounding area. In the former case, a "Stroke Identification" operation (including an

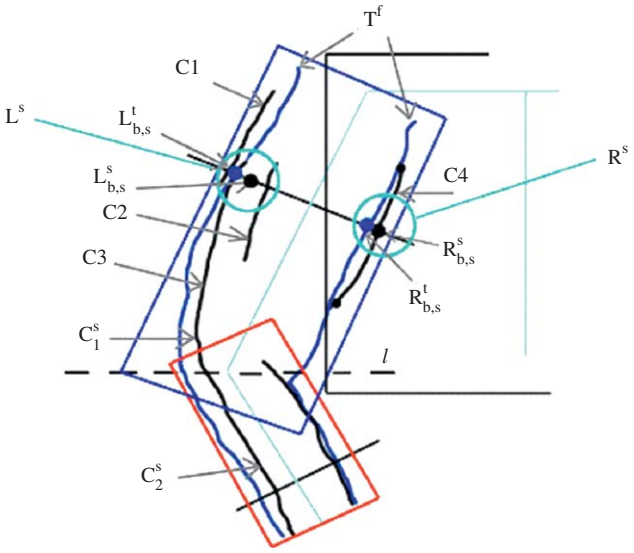

Fig. 8. 2D raw sketch processing. For the multiple strokes C1, C2, and C3, an average point $L_{b,s}^s$ is computed among the corresponding sectional intersection points. The stroke C4 is located in both the upper torso and upper arm bounding area. After "stroke identification", it is assigned to the upper arm due to a minimum in-between angle with the upper arm rather than the upper torso. A long stroke C3 is first segmented into stroke C_1^s and C_2^s (through "stroke segmentation"), which are further checked upon the locating bones.

orientation check followed by a *distance check*) is performed to identify the candidate bone which is most likely to be rendered. This bone has a closer orientation and/or distance to a given stroke. In the latter case, a "Stroke Segmentation" operation is performed to segment a long stroke into separate pieces by using mid-lines of the joint angles that are in-between pairs of neighbouring bones spanned by the stroke. Next, the segmented strokes are further processed to identify their locating bones. A detailed description of "Stroke Identification" and "Stroke Segmentation" methods is included in the Appendix of this paper.

6.2. Rigid morphing and body feature point extraction

As illustrated in Fig. 7, once the user completes a figure sketch and selects to reconstruct it into a 3D body model, an automatic system process starts for rigid morphing, fatness morphing (Section 6.3), and surface matching (Section 6.4). As previously mentioned, rigid morphing comprises two steps: 1) deform the original 3D generic model against the body proportion of the sketched figure; 2) deform the scaled generic model against the reconstructed body posture of the sketched figure. Here, when a bone segment is scaled up or down, its cross-section in-between distances are changed whilst the size and fatness value (sectional/angular fat and overall area) of each cross-section is preserved. Thus, the sectional fat distribution value $D_{b,s} = P_{b,s}/P_b$ ($s = 1,2, \ldots, n$) of the given body part is re-computed, since its fat percentage P_b has changed (whilst its sectional fat percentage value $P_{b,s}$ stays invariant).

After rigid morphing, the updated 3D template is projected onto 2D (*XY* plane) to obtain the body silhouette and a set of 2D cross-section lines (projected from template cross-section slices). Here, the extracted silhouette is segmented into each individual body part. Then, indexed intersection points (template feature points) are found between 2D cross-lines and the parsed template silhouette. For each body part, left and right feature point lists (L^t and R^t) are automatically sorted by body part index b ($b = 1,2, \ldots,12$) and cross-section index s ($s = 1,2, \ldots, n$), where n varies for different body parts. Finally, this *template feature point* set is saved as $T^f[L^t_{b,s}, R^t_{b,s}]$.

Similarly, intersection points can be found between saved sketch strokes and template cross-lines. For each bone cross-line, all the associated (previously labelled) rendering strokes are retrieved to obtain a set of sectional feature points. Then, these points are further grouped as L^s and R^s according to their interface locations (see Fig. 8). Here, each feature point group (L^s or R^s) contains multiple points because of multiple/overlapping sketch strokes. Next, an average point is computed for each feature point group. They are saved into $L^s_{b,s}$, $R^s_{b,s}$ representing the principal feature points of this sketch cross-section. Finally, a *sketch feature point* set $S^f[L^s_{b,s}, R^s_{b,s}]$ is extracted by performing this operation for each cross-section on each body part.

For the body parts with discontinuous contours (e.g. the left lower torso in Fig. 7a), feature points in L^s and/or R^s may be partially missing. In this case, the system distinctively labels the unfilled points in their indexed feature point list to indicate this status.

6.3. Fat distribution estimation and fatness morphing

The rigid-morphed 3D template model (see Fig. 7a) is used to estimate the body part fat percentages of the 2D sketched figure. Here, we assume that when a body fattens/slims, its inner volume stays relatively unchanged compared with the fat volume. That is, for each body cross-section, only its overall area enlarges when new fat accumulates whilst its inner area stays invariant. In this sense, the fat percentage of each body part on a 2D figure drawing can be estimated through graphical comparison. As shown in Fig. 9, since the template inner area S^i and outer area S^o are known for each cross-section, a new outer area $S^{o\prime}$ can be calculated for the given cross-section through $S^{o\prime} = S^o(D^s_{c,s}/D^t_{c,s})$ (whilst $S^{i\prime} = S^i$). $D^s_{c,s}$ and $D^t_{c,s}$ here stand for the corresponding cross-line lengths on the 2D template and sketched figure, which can be obtained by computing the distance between the previously extracted sketch feature points ($L^s_{b,s}, R^s_{b,s}$) and the template feature points ($L^t_{b,s}, R^t_{b,s}$). For some cross-sections that have missing sketch points, $D^s_{c,s}$is set to be equal to$D^t_{c,s}$. After getting the $S^{i\prime}$ and $S^{o\prime}$ for each cross-section, a new body part fat percentage P_b' can be obtained by Eq. (5), given a set of known cross-section in-between distances. Through this graphical comparison process, body part fat percentages (body fat distribution) across the whole body can be estimated for the 2D sketched figure. A fatness morphed model (see Fig. 7b) can be achieved through deforming the rigid-morphed generic model according to the pre-defined body-fattening scheme (described in Section 5.4), given a set of new fat percentage inputs. As illustrated, after fatness morphing, the 3D body is "physically" transformed with fattened belly and thighs.

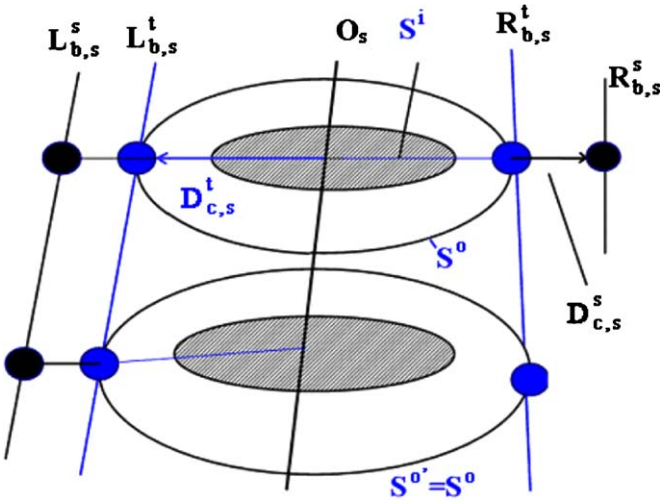

Fig. 9. Fat distribution estimation.

6.4. Surface matching and 3D model auto-beautification

After automatic rigid and fatness morphing, the appearance of the original 3D template gradually approaches that of the 2D sketched figure. However, it still does not fully match the 2D drawing (see Fig. 7c), since its general body shape is inherently constrained by the original generic model physiques. Thus, "surface matching" needs to be performed to make the projection of the 3D model identical to the 2D sketch. Since natural freehand sketches are featured by roughness and imperfections, a complete matching may lead to an implausible and even distorted 3D body. In reality, when people observe a figure sketch, their brains can envision a regular human body despite imprecise 2D features. Thus, a computer should also be able to emulate this figure "auto-beautification". Moreover, users may sometimes prefer a rather crude and casual-looking model, which conveys the original style and characteristics of their figure sketch. Hence, the system requests the user's choice here to allow a figure "auto-beautification" via an interactive dialogue window.

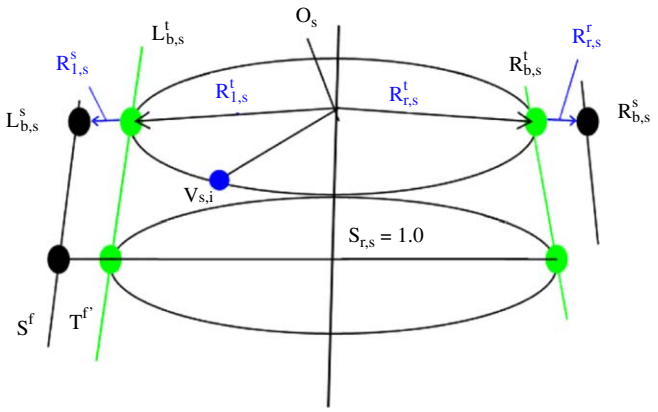

Fig. 10. Retrieve the surface matching measurements.

Fig. 10 demonstrates how the system automatically performs an exact surface matching. First, it extracts the silhouette feature points $T^{f'}[L^t_{b,s}, R^t_{b,s}]$ from the fatness morphed 3D template. Then, $T^{f'}[L^t_{b,s}, R^t_{b,s}]$ is compared with the saved sketch point set $S^f[L^s_{b,s}, R^s_{b,s}]$ against the radii (template radius:$R^t_{l,s}$,$R^t_{r,s}$, sketch radius: $R^s_{l,s}$,$R^s_{r,s}$) from the sectional ray centres (O_s) to the corresponding leftmost and rightmost feature points. After that, to match the template contour to the sketch contour, scale measurements $S_{l,s}(S_{l,s} = R^s_{l,s}/R^t_{l,s})$ and $S_{r,s}(S_{r,s} = R^s_{r,s}/R^t_{r,s})$ are taken. These measurements are further linear interpolated to get the scale factor $S_{s,i}$ (s: section index, i: ray index) for each sectional ray. Here, the corresponding scale value is set to 1.0, where there is an unfilled feature point. Then, given the ray centre O_s, scale value $S_{s,i}$, and the associated template vertex $V_{s,i}(x,y,z)$, a new skin vertex position $V'_{s,i}(x', y', z')$ is computed through $V'_{s,i} = S_{s,i}(V_{s,i} - O_s) + O_s$. Repeating this process on each template cross-section results in an updated skin mesh, whose 2D profile matches the figure sketch completely. Fig. 7c shows the 3D model after exact matching.

For 3D model auto-beautification, the system averages the sectional scale factors between the left and right torso and between the left and right limbs, based on the pre-computed scale measurements $S_{s,i}$. For a sketched figure whose left and right body postures are different (e.g. left arm straight, right arm folded up with muscles drawn inflated), the current auto-beautification method is still generally applicable, since the scaling measurement $S_{s,i}$ here is computed based on the silhouette of the sketched and template body, where the template body has been deformed accordingly to the current body posture for acquiring the appropriate scaling measurement. The system then applies this new scale set $S'_{s,i}$ to the fatness morphed 3D template (in its original pose where the left and right sides of the body are symmetrical) to attain the beautified model, which can be posed into the sketched body pose again to achieve the final mesh model. Fig. 7c shows the resulting 3D model after the body beautification.

6.5. 3D figure modifications through 2D contour over-sketching

After above processing, users are given a plausible 3D character model, which is reconstructed from the initial freehand sketch. Then, this 3D model can be globally refined by over-sketching its 2D figure profiles (see Fig. 7d). The above-mentioned sketch processing is performed again when the user over-sketches figure contours and selects to reconstruct the 3D human body model.

7. Sketch-based local skin surface modification

We studied a sketch-based method for local skin surface deformation by means of drawing a suggestive contour and a view-dependent silhouette contour (see Fig. 11). Given a sketch-generated 3D human body displayed on the interface, the user firstly selects a body part (e.g. upper torso) to be modified. The system automatically aligns the inner skeleton of this body part to the global Y-axis. The user then sketches a *suggestive contour stroke* on the skin surface to convey the local surface shape. This suggestive stroke is represented as a curve in the screen space ($Z = 0$). Next, the user rotates the given body part along the Y-axis to choose an editing viewpoint (the sketched suggestive contour is transformed during the rotation). Then, the user draws a new *silhouette contour stroke* (also represented as a curve in the screen space) near the transformed suggestive contour to depict a profile of the local surface surrounded by the suggestive contour. When the user selects to view the skin modification results, the system first calculates the Region of Influence (ROI) to be deformed and the ray scaling factor of each influential mesh point. A new mesh point position is then computed, given the ray centre coordinates (of the cross-section it lies on), its original point coordinates, and its assigned ray scaling factor. The local skin surface is deformed by updating all mesh point positions in the identified ROI. As shown in Fig. 11 the user can sketch the skin feature (e.g. right chest) on one side of the body and mirror it on the other side (e.g. left chest) without specifying it on each side.

7.1. Identify the Region of Interest

As previously introduced, the sketch-generated models in our system share the same mesh structure: cross-sections centred along the inner skeleton and indexed casting points (*40* for *torso*, *36* for *limbs*) lying along the edge of each cross-section slice. Then, if fixing the rotation angles α to be $m \times A_i$ (*torso*: $A_i = 9^\circ$; *limbs*: $A_i = 10^\circ$; $m = 0, \ldots, n$) when rotating a body part along its bone axis (Y-axis) from an original view, its silhouette in a new viewpoint is a polyline running through a column of mesh points (named *silhouette column*, illustrated in black in Fig. 12a), whose column index c (*torso:* $c = 0, \ldots, 40$; *limbs:* $c = 0, \ldots, 36$) can be calculated given the initial viewpoint and rotation angle of the model (see Fig. 12a). This silhouette is treated as a *source silhouette*, which lies on the same image plane ($Z = 0$) as the *silhouette contour stroke* (*target stroke*, illustrated in blue in Fig. 12a) the user has drawn in the screen space. Then, given the 3D coordinates (X/Y: extracted from the drawing, $Z = 0$) and the rotation angle α, the far end point P^c of the silhouette stroke (the point that is the furthest point on the silhouette contour stroke from the bottom of the transformed suggestive contour stroke, $P^{c\prime}$s position is illustrated in Fig. 12a) can be transformed back to the original model view, where the *suggestive contour stroke* has been drawn. Here, a *suggestive contour stroke* is a curved stroke that the user draws on the skin surface (in the screen space, $Z = 0$) to convey the local surface shape (illustrated as a green curve in Fig. 12a). Since the suggestive contour is mostly an open curve, we devised a simple way to get the ROI boundary (If the suggestive contour is a closed curve, this curve itself is the boundary of the ROI.). For the former case, given the start and end point (P^s and P^e) of the suggestive contour and the transformed P^c of the silhouette contour, a circular curve is fitted to run through these three points. This curve linked with the suggestive contour curve is considered as the boundary of the ROI (see Fig. 12b). Here, some interpolation points are set in-between P^s and P^c, and P^c and P^e on the circular curve.

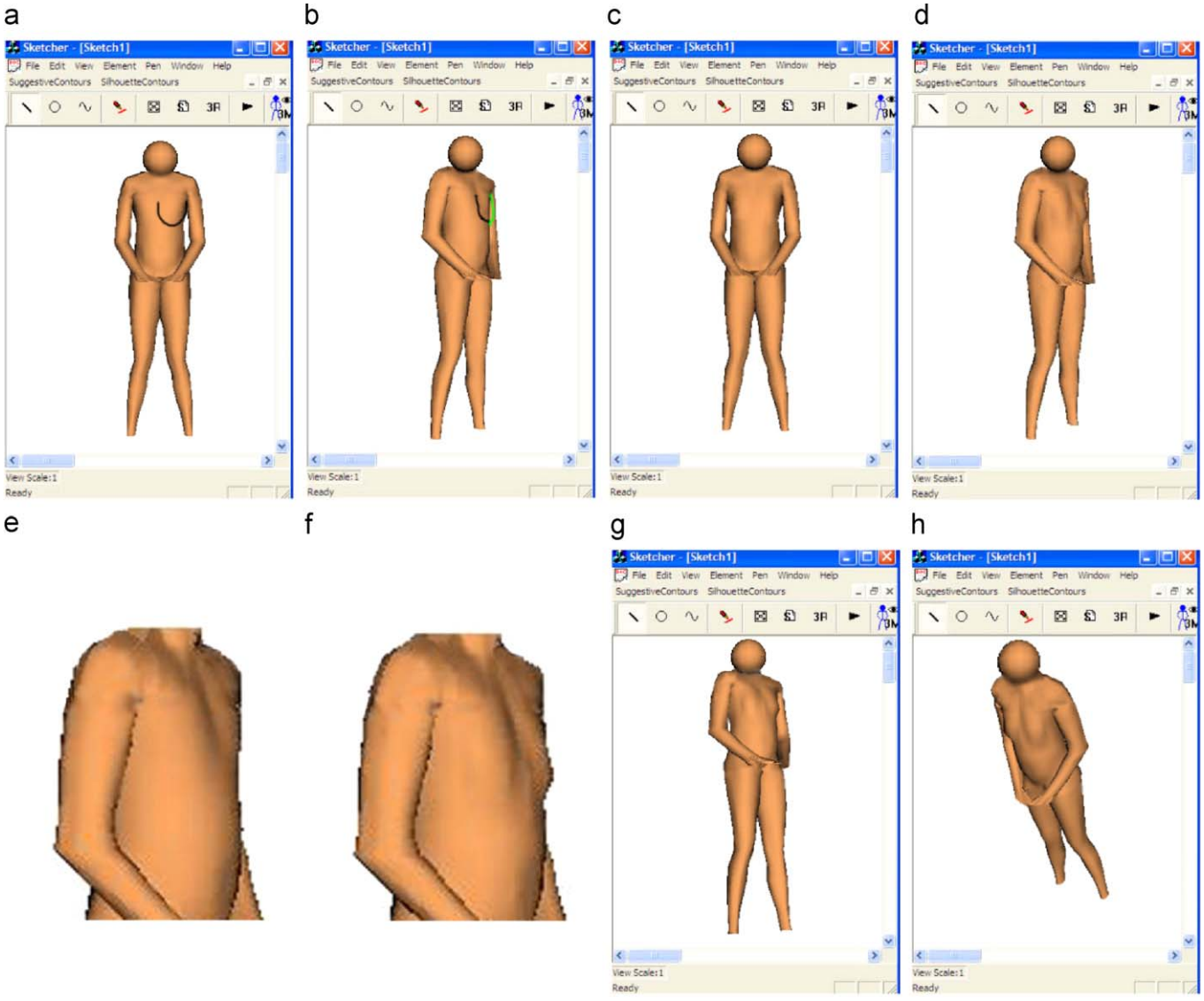

Fig. 11. (a) Drawing a suggestive contour on the skin surface to depict the shape of the chest. (b) Drawing a silhouette contour near the transformed suggestive contour to specify the new profile of the chest. (c and d) The front/rotated view of the model with the deformed chest and mirrored-up effects. (e) The original chest surface. (f) The transformed chest surface. (g and h) The updated body model from different viewpoints.

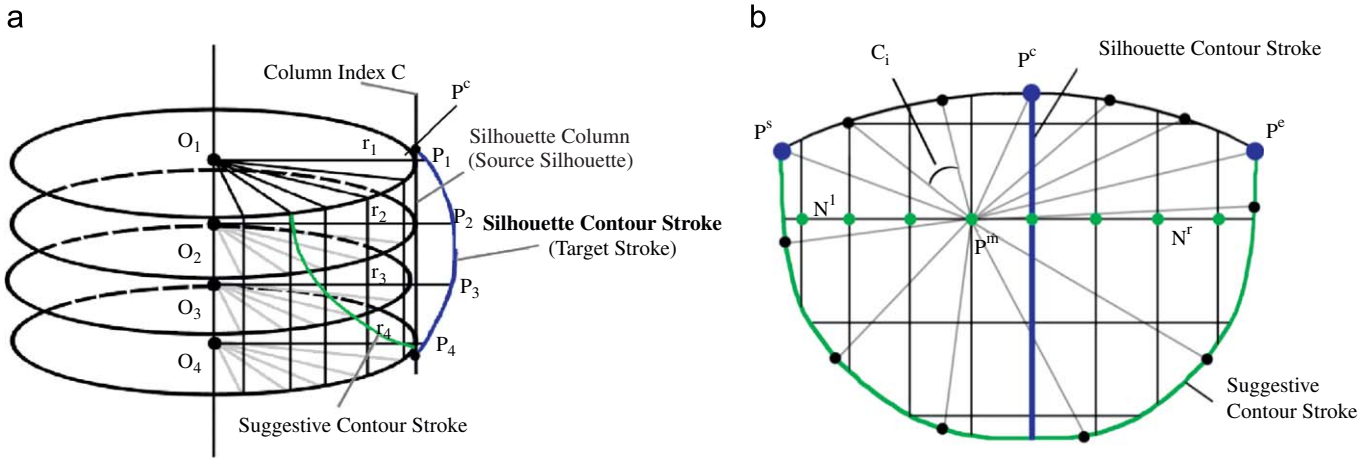

Fig. 12. (a) Silhouette column (black), silhouette contour stroke (blue), and suggestive contour (green) stroke on the mesh surface. (b) Identified ROI boundary and ROI points. (For interpretation of the references to colour in this figure legend, the reader is referred to the web version of this article.)

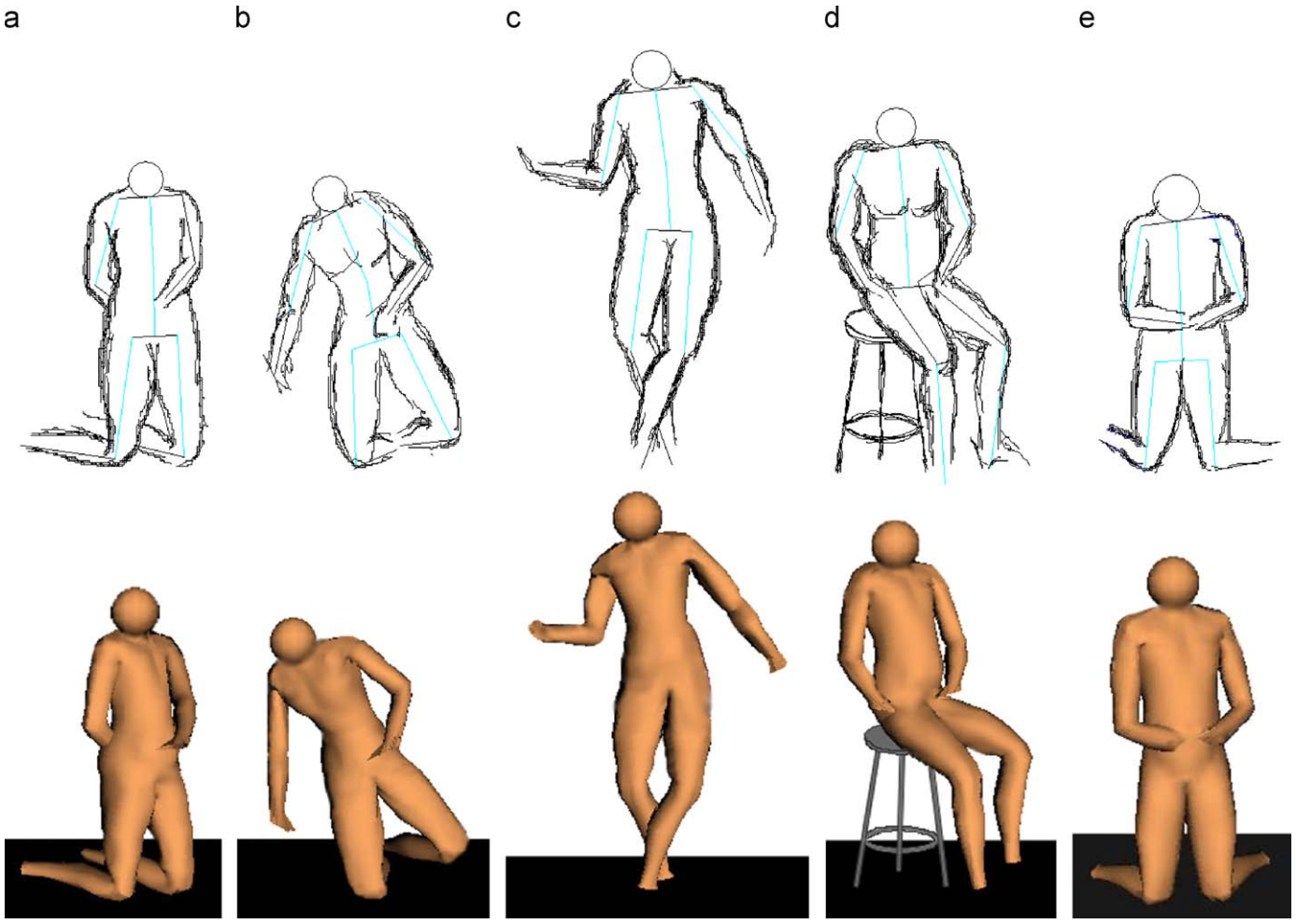

Fig. 13. Freehand figure sketch input and the reconstructed 3D human body models in various figure postures, drawing views, and body shapes.

To identify the mesh points located inside the ROI boundary, each mesh point P^m (on the edited body part) is checked through the following steps (See Fig. 12b): (1) project P^m and the identified ROI boundary points onto the XY plane (keep its X/Y value and discard its Z value); (2) link P^m to the ROI boundary points and get the angle C_i ($i=0,\ldots,n$; n is the number of points on the ROI boundary curve) in-between each pair of neighbouring link lines; (3) accumulate all in-between angles to get a sum angle S ($S=\sum_{i=1}^{n} C_i$); (4) if S value is within an angle range [360°−10°, 360°+10°] (10° is a adjustable heuristic value), the point P^m is considered to be an influential point inside the ROI boundary; if not, it is regarded as outside the ROI boundary. Once identified as an influential point, the point index of the given point is recorded. Moreover, the number of the ROI points on the left and right side (N^l and N^r) of the *Silhouette Column* on each layer is recorded, since each point of the *Silhouette Column* is one of the influential mesh points located on a cross-section layer (see Fig. 12b).

7.2. Calculate the ray scaling factors of ROI points

As shown in Fig. 12a, since the source and target silhouettes are located on the same image plane, the new mesh points P_s on the target silhouette are the intersection points between the cross-section rays (which run through the corresponding ray centres O_s and the silhouette column points) and the target silhouette curve. Then, the ray scaling factor S_s of a silhouette column point can be computed through $S_s=(P_s-O_s)/r_s$, where r_s is the ray radius of the given silhouette column point. Next, given the previously recorded N^l and N^r value and the S_s value (of the silhouette column point) for each cross-section layer, the ray scaling factors ($S_{s,i}$) of other influential points on this layer are computed through a *Hermit spline interpolation* (discussed in Appendix). Repeating this process for each influential layer generates the ray scaling factors of all influential points within the ROI. Finally, given a sectional ray centre, the original point coordinates, and its ray scaling factor, an influential point position is updated. The local skin surface is deformed by updating the positions of all mesh points in the given ROI.

If in the case that the user selects to mirror the skin features from one side of the body to its symmetrical side, the system firstly computes the influential point indices in the opposite ROI based on those in the original ROI and the cross-section point indexing sequence (see Fig. 4d). Then, the ray scaling factor of each influential point in the original ROI is assigned to its counterpart point in the opposite ROI. Finally, the local surface in the opposite ROI is deformed following the same routine as described above.

As shown in Fig. 11, our current method enables users to sketch-out local skin features such as chest muscles. There are, however, difficulties in modelling subtler body features such as a navel due to the current mesh density. This method can be joined with other sketch-based surface deformation methods [26,28] to

model more varieties of skin features such as the shape of prominent bones and blood vessels on the skin surface.

8. Results and discussion

This section presents and discusses current results on sketch-based human body modelling and animation and 3D body generation through direct generic model manipulation and morphing. Moreover, we compare our VHS with other modelling systems and propose the potential application areas of our current human modelling/animation techniques and system.

8.1. Sketch-based human body modelling and animation results

As shown in Figs. 13 and 14, our sketch-based modelling interface VHS transfers users' freehand figure sketches into plausible 3D human models of various body proportions, shapes, and postures. After illustrating a stick figure posture, users can flesh it out in flexible drawing sequences with natural and artistic contour strokes, like drawing on an electronic canvas.

Fig. 13 shows a series of freehand figure sketches (featured by multiple/overlapping strokes, body part foreshortening/occlusion, and drawing imperfections) and their 3D counterpart models in a mixture of figure postures (e.g. Fig. 13a and e—kneeling, Fig. 13b—picking, Fig. 13c—dancing, and Fig. 13d—sitting), drawing views (e.g. Fig. 13a and d—side views, Fig. 13b, c and e—front views), and body shapes (varied body proportions and fat distribution). Our system can handle a figure sketch with foreshortened body parts thro, c and d), human joint ROM, and key frame coherence are utilised for 3D pose recovery. Moreover, our system can handle figure sketches with large overlying areas as shown in Fig. 13a–c and e. Here, the occlusion order of the overlying body parts is solved by identifying the orientation of foreshortened body parts. The problem of missing body contours is handled by labelling the unfilled sketch feature points and processing them specifically during template morphing.

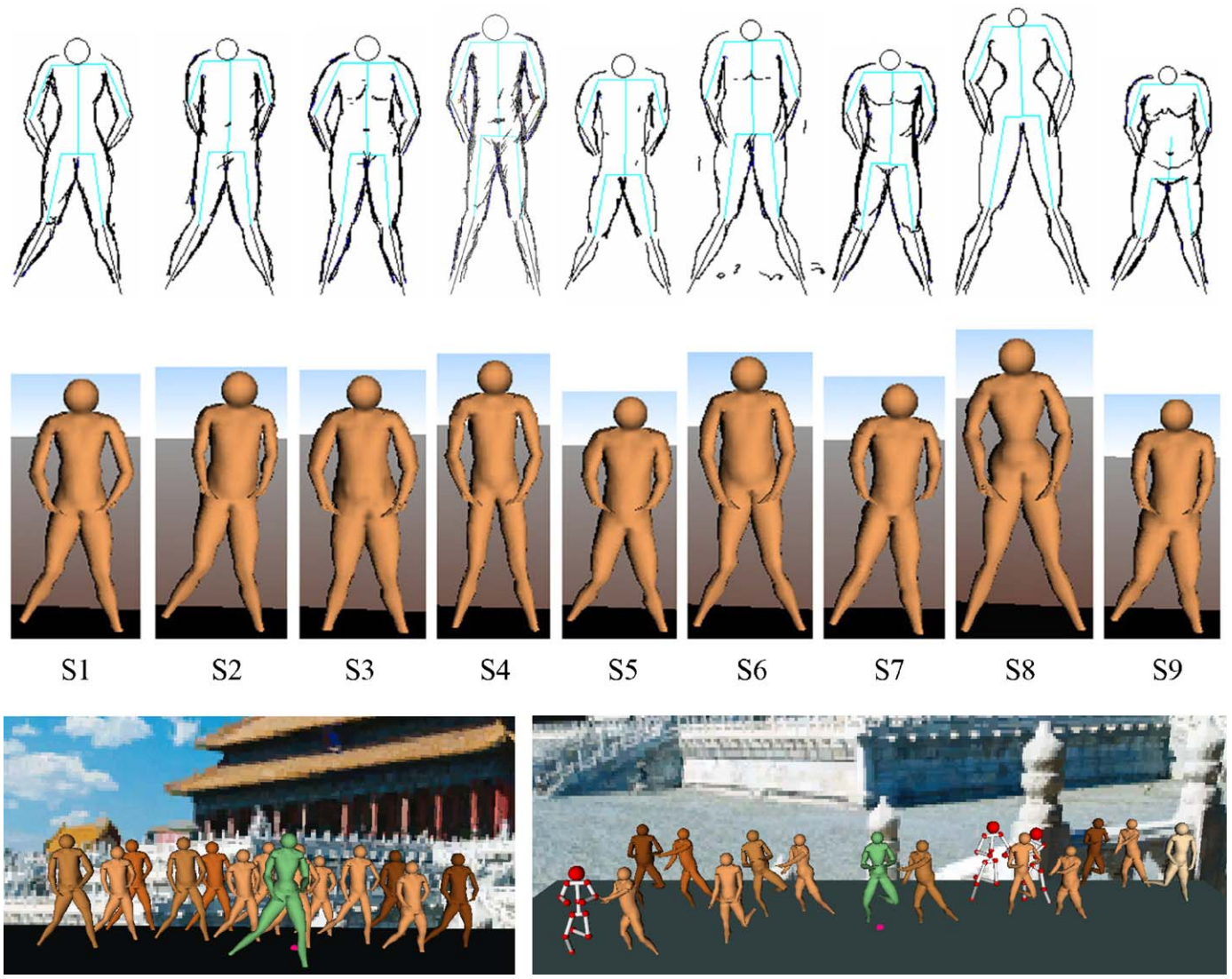

Fig. 14. (Top) A variety of 3D virtual humans and the original drawings created by different users: an artist (S3), a designer (S4), an animator (S6, S7), graduate students (S1, S2, S5, and S9), and a child (S8). Here, all 3D models appear to have a similar front view posture because the users were required to draw the predefined figure key frames for the measurement of their drawing performance. (Bottom left) A population of user-created 3D virtual humans (skin colours varied by authors) are playing Chinese Kungfu together in a vivid 3D world with music (the pink ball on the ground is a music trigger). (Bottom right) A crowd of virtual humans and stick figures are fighting with each other in a 3D virtual world. Two of them (the 5th from the left, and the furthest right figures) are performing different actions. This shows individuality among the collective behaviour.

Table 1
Software comparison: learning time and actual modelling time.

Time	Teddy	Virtual Human Sketcher	3DS MAX (average)	Poser
Software learning time	15 min	15 min	3 h	2 h
Modelling time	50 min	18 min	6–8 h	1 h

Fig. 14 (top) shows a range of human body shapes (e.g. apple, pear, hourglass, rectangle, etc., with distinct body sizes and fat distributions) and even a super human model (S8) generated by different users (an artist, a design student, an animator, graduate students, and a 12-year-old child) in a user evaluation for VHS (briefed in Section 9). These sketch-generated virtual humans are readily animatable and are integrated in an interesting Chinese Kungfu animation (see Fig. 14 (bottom left)), where the body motions are defined by sketch-based stick figure key framing (Section 3) and motion retargeting. Fig. 14 (bottom right) shows a group of virtual humans and stick figures Kungfu fighting with each other. This multi-actor fighting motion is generated through our sketch-based storyboarding method detailed in [21].

As shown in Figs. 13b and d, and 14 (S3, S4, S6, S7, and S9), inner contours are added by users on some sketches after 3D model generation (since these models were created before the implementation of our sketch-based skin modification method). This shows their intention to depict local surface features through more rendering forms (e.g. suggestive contours). Note that, some reconstructed 3D models (in Fig. 14) in slightly unnatural postures are created from users' imprecise figure sketches. These "invalid" figure poses can be adjusted by our "overall pose checking and auto-correction" routine.

Compared with normal creative methods [1–3], our method enables users to generate 3D human bodies through 2D figure sketching, which is particularly fast and easy for ordinary users. Different from the reconstructive approaches [6,7], which require multiple orthographic images to recover the 3D geometry of an existing person, our method enables the transformation of a single raw figure sketch (inherently noisy and imprecise) into an imaginative 3D human body model. Moreover, unlike a purely geometric mapping of 2D extracted features onto a 3D generic model [6], our method is novel, because it can estimate the fat distribution condition of a sketched figure and morph the 3D template both geometrically and somewhat physically to achieve a moderately plausible human body model. Although [12] introduces the overall body fat percentage and hip-to-waist ratio to modify a global body shape, human bodies are essentially varied in each individual body part, which is difficult to represent by general sizing parameters. In contrast with [10,12], which request the user's numerical anthropometrical input, our system interprets the graphical configurations directly from the user's figure sketches to materialise their intended 3D characters. In this sense, a superhuman-like model (see Fig. 14) can be created by our sketching interface. This is instead difficult to achieve with an example-based method [5,10–12].

8.2. Comparison to existing systems and potential applications of Virtual Human Sketcher

To compare VHS with other sketching systems and commercial 3D modelling software, we conducted a simple user testing in which one design student is asked to create a 3D human body model in a "sitting" posture using Teddy system [13], VHS, and 3DS MAX respectively; another design student is asked to create the same "sitting" model using Poser; and four other design students are asked to create 3D models in the similar postures as those in Fig. 13a–c, and e using 3DS MAX. All of these users have no previous experiences with any of these modelling tools. In order to measure and compare the software learning time and modelling time easily, users are asked to firstly learn the corresponding modelling functionalities and then to create a 3D model at approximately the same level of details (LOD) using aforementioned modelling tool(s) respectively. The recorded software learning time and modelling time are displayed in Table 1, and the resulting human body models are shown in Figs. 15 and 16.

Note that, the user testing here mainly aims to provide a quick and approximate comparison of the timing and process of creating 3D models by utilising VHS and other 3D modelling systems. In Section 9, a more in-depth user testing on VHS itself has been briefly introduced, involving 10 different users, various modelling tasks, and a variety of evaluation methods (including performance tests, sketching observation, and user interviews), More details on our user tests and studies, as well as our user-centred and scenario-based design approaches, have been presented in [37]. A more formal and comprehensive comparison study, which involves more users of different levels of skills and includes more modelling tasks (e.g. pose definition, global body modelling, and local surface modification) is going to be conducted in the future.

With a simple and intuitive user interface, Teddy requires only 15 min software learning time. However, since Teddy enforces a "part-by-part" drawing routine and only accepts single stroke input, the user needed to model the torso first and then extrude each body part from another by drawing a closed base stroke and a silhouette stroke to specify the shape of the corresponding body part. Since Teddy cannot handle body part foreshortening and occlusion, the user needed to always rotate the model to bring the base stroke sideways and then draw the silhouette line to extrude the surface. Requiring a series of extrusion, cutting, smoothing, and transformation operations, the modelling process using Teddy is more like assembling a handcraft toy with gestures rather than natural freehand sketching. Although taking nearly 50 min modelling time, the resulting 3D body model (see Fig. 15a) appears coarse, stuffed, and lacks of local surface details. It shows that current sketching systems [13–15,25,26] (represented by Teddy) are not suitable for sketching out plausible virtual human models, constrained by their underlying construction schemes and application context.

3DS MAX has a complex WIMP-like (Windows Icons Menu Pointer) graphical interface. It took users averagely 3 h to learn basics of the 3D modelling process, specialised modelling concepts and terminology (i.e. primitives, subdivision, control points, etc.), various modelling/editing operations (i.e. extruding, sculpting, refining, etc.), and interface menus/toolkits. During the 3D body modelling process, users needed to start modelling a body part (i.e. torso) from a geometry primitive (i.e. cylinder), and then perform a series of extruding (extruding polygons), subdividing, sculpting (sculpting the newly generated geometry by moving vertices, edges, and polygons), and refining operations to transform a geometry primitive into a desired shape. Each new body part is created by extruding from the existing ones according to the human body topology. The whole modelling process is long

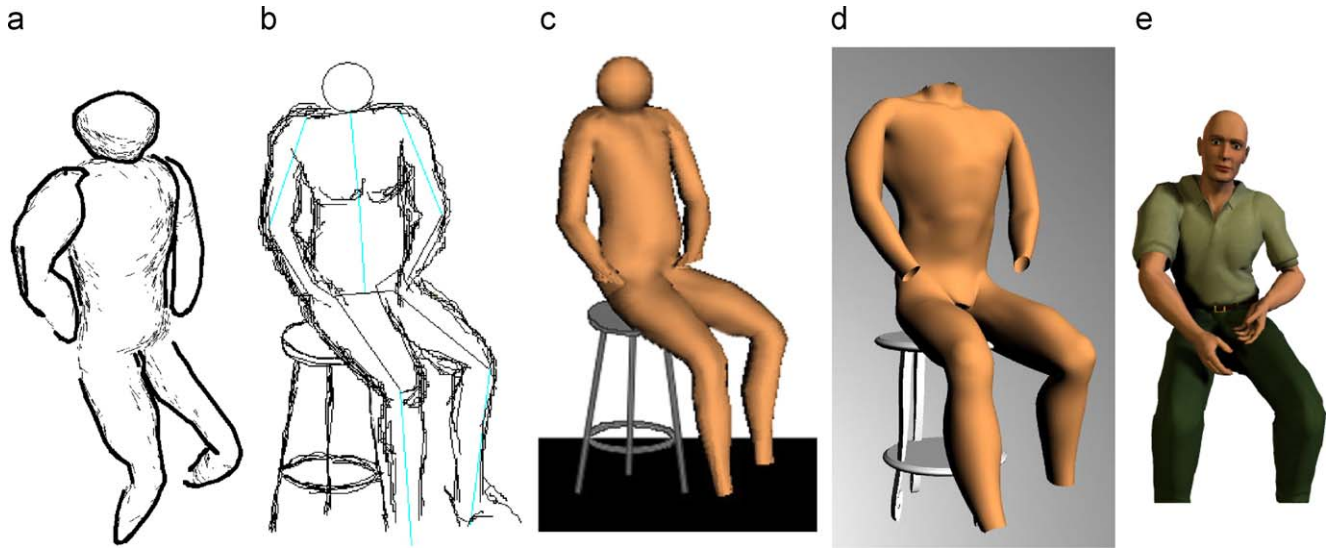

Fig. 15. (a) 3D model generated from Teddy system; (b) 2D freehand sketch input of Virtual Human Sketcher; (c) 3D model generated from Virtual Human Sketcher; (d) 3D model generated from 3DS MAX; (e) 3D model generated from Poser.

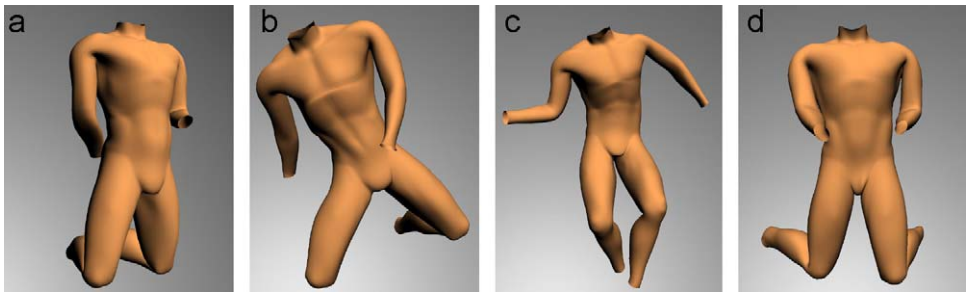

Fig. 16. 3DS MAX generated models in the similar postures as those in Fig. 13a–c and e.

and demanding, it took the (first-time) user(s) nearly 8 h to create a 3D "sitting" model and averagely 6–8 h to create other 3D models in various postures with medium LOD (see Figs. 15d and 16) using 3DS MAX.

Poser 7 is specialised software for 3D figure design and animation. Users can load a poser template figure from the figure library. A Poser figure consists of named body parts that can be selected and articulated (or posed). Users can use camera operations to change views and use edit tools to select a body part and move it to a desired position. The use of Poser can make a posture by interactively changing each individual body part. This process, however, still takes time (learning and modelling time) to get a good pose, while VHS requires less software learning time and can enable users to intuitively sketch-out a 3D human body and reconstruct the body pose approximately in a semi-automatic manner with less time.

Similar to Teddy, VHS is easy to learn and requires minimum training time. It took the user 15 min to grasp basics of the "Stick Figure→Fleshing-out→Skin mapping" modelling pipeline and functions for sketch-based stick figure posing as well as full figure Fleshing-out. The sketch-based modelling process is fast and straightforward. After specifying the stick figure posture, the user fleshed it out with multiple freehand strokes in a flexible drawing sequence. It took the user only 18 min to sketch-out a plausible 3D "sitting" model with medium LOD including its underlying 3D stick figure model (see Fig. 15b/c). The resulting 3D model is automatically skinned and is readily animatable in both our system and other commonly used animation systems. Details of a more formal user testing that we have conducted with 10 different users on VHS are presented in Section 9.

Compared with Teddy and other similar sketching systems, we devised a unique and specialised solution for addressing the challenge of transferring a single freehand figure sketch into a plausible 3D human body model through using a "Creative Model-based Method", which is inspired by the hints and elements of human perception and utilises a 3-layered generic model to interpret the physical attributes (body size, shape, fat distribution) conveyed by a sketched figure and to create a 3D counterpart model through graphical comparisons and generic model morphing (rigid morphing, fatness morphing, and surface matching). Specialised in human body modelling and animation, our system contains the pre-knowledge of human body joint range of motions and inner body layers, and can create animatable 3D human models with plausible body poses and various body shapes influenced by the variation of inner body layers.

Compared with 3DS MAX, Poser, and other commonly used 3D commercial modelling software, VHS has an intuitive sketching interface, which is easier to learn and use. It enables the user to rapidly create 3D human body models with intermediate LOD through freehand sketching, which is a natural, intuitive, and flexible medium for all level of users. As shown in Table 1, Fig. 15, the user spent only 15 min learning time and 18 min modelling time to sketch-out a 3D "sitting" model with intermediate LOD, whilst it took the user 3 h learning time and 8 h modelling time to create a 3D model with similar LOD using 3DS MAX by sculpting from geometric primitives. The use of Poser took the user 2 h

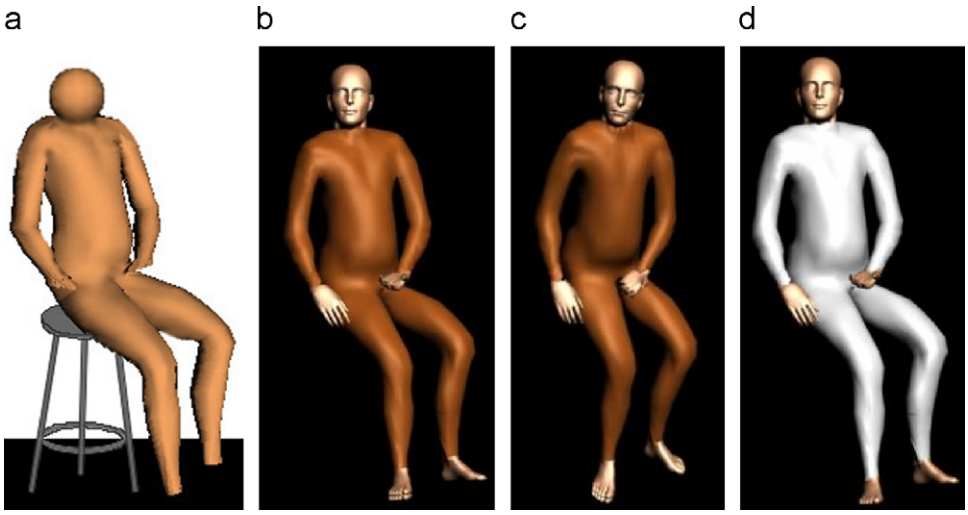

Fig. 17. (a) The 3D model generated by Virtual Human Sketcher originally. (b and c) The intermediate 3D model generated by Virtual Human Sketcher can be further enhanced into a plausible 3D human character through surface smoothing (in Geomagic) and adding higher level details such as head, hands, feet, etc. (in 3DS MAX). (d) The clothed 3D character after modifying the body surface colour.

Table 2
Original fat percentage value of each individual body part on the 3D generic model.

Upper arm	Lower arm	Upper leg	Lower leg	Upper torso	Lower torso	Shoulder
32.2059	23.4728	33.3846	24.1899	18.7302	37.6321	18.6134

learning time and 1 h to model a similar pose. The modelling time here is shorter comparing to 3DS MAX because Poser is specialized software for human pose design using figure templates.

This suggested that VHS can be utilised as a rapid prototyping tool to quickly sketch-out intermediate 3D human body models, which can be exported into commercial software (e.g. 3DS MAX), for modelling higher level surface details and for creating realistic 3D human characters as end products. Fig. 17 demonstrates how an intermediate human body model sketched out from VHS can be further enhanced by Geomagic (reverse engineering software) and 3DS MAX into a believable 3D human character through surface smoothing (in Geomagic) and adding/editing higher level details such as head, hands, feet, clothes, muscles, etc. (in 3DS MAX). Featured by its fast and intuitive sketching interface, VHS could potentially be developed into a plug-in to commercial packages for rapid 3D human body prototyping, since it can considerably shorten the time of generating human models with intermediate LOD through traditional 3D sculpting, which is normally based on geometric primitives. Meanwhile, VHS stands alone as a fast, easy, and low-cost human modelling and animation tool, which enables users to generate simple 3D stick/full figure models and animations through freehand sketching, using a "Stick figure→Fleshing-out→Skin mapping" modelling routine. Moreover, VHS can benefit non-professional users as a casual entertaining tool, which enables anyone, who can draw, to create their own 3D characters and animations easily and enjoyably. The current VHS and its underlying techniques can be further developed to improve its modelling and animation quality. The discussion on the related future work is presented in Section 10.

8.3. 3D body models generated by direct manipulation of body fat percentage value

Apart from integrated in a sketch-based modelling application, our multi-layered template acquisition and morphing scheme can stand alone as a body-enrichment technique to generate a variety of new human body shapes for common applications, where body parameters (body proportions, body part fat percentages, etc.) can be directly manipulated. Similarly, the generated 3D body models can be exported into commercial packages for modelling higher level details.

Table 2 presents the actual fat percentage value of each template body part evaluated through body fat distribution digitisation of the VHP template model. Fig. 18 shows a range of limb (arm/leg) models after fatness morphing, given varied upper and lower limb fat percentage value. The fat percentage input (0–100%) here is a normalised value referring to the actual template fat percentages.

Given a single template model and its digitised body fat distribution value, Fig. 18 shows how direct manipulation of inner body fat percentages can generate a variety of new body shapes ranged from muscular to medium to overweight without resorting to any additional examples. It also shows how the variation and control of inner body layers (such as the fat layer) can effectively and dramatically transform the outer appearance of human bodies. In other words, integration of more physical layers adds more dimensions of flexibility, information, and control in creating varied human bodies of plausible physical attributes. The close-up views of newly generated limb models demonstrate the effects of our fatness morphing scheme when utilised to "physically" fatten the body models, which resulting in apparent transition and changes of physical body features. As shown in Fig. 18, distinct skin texture (fat-stuffed, muscular-tight) and local surface details can be observed from the resulting limb models. These physical attributes cannot be easily achieved by purely geomeric scaling of template models. Although there are some unrealistic deformation exhibited around the elbow area of some fatness morphed arm models in Fig. 18, it could be improved by surface smoothing around the body joint area where body parts of different body fat percentages are connected.

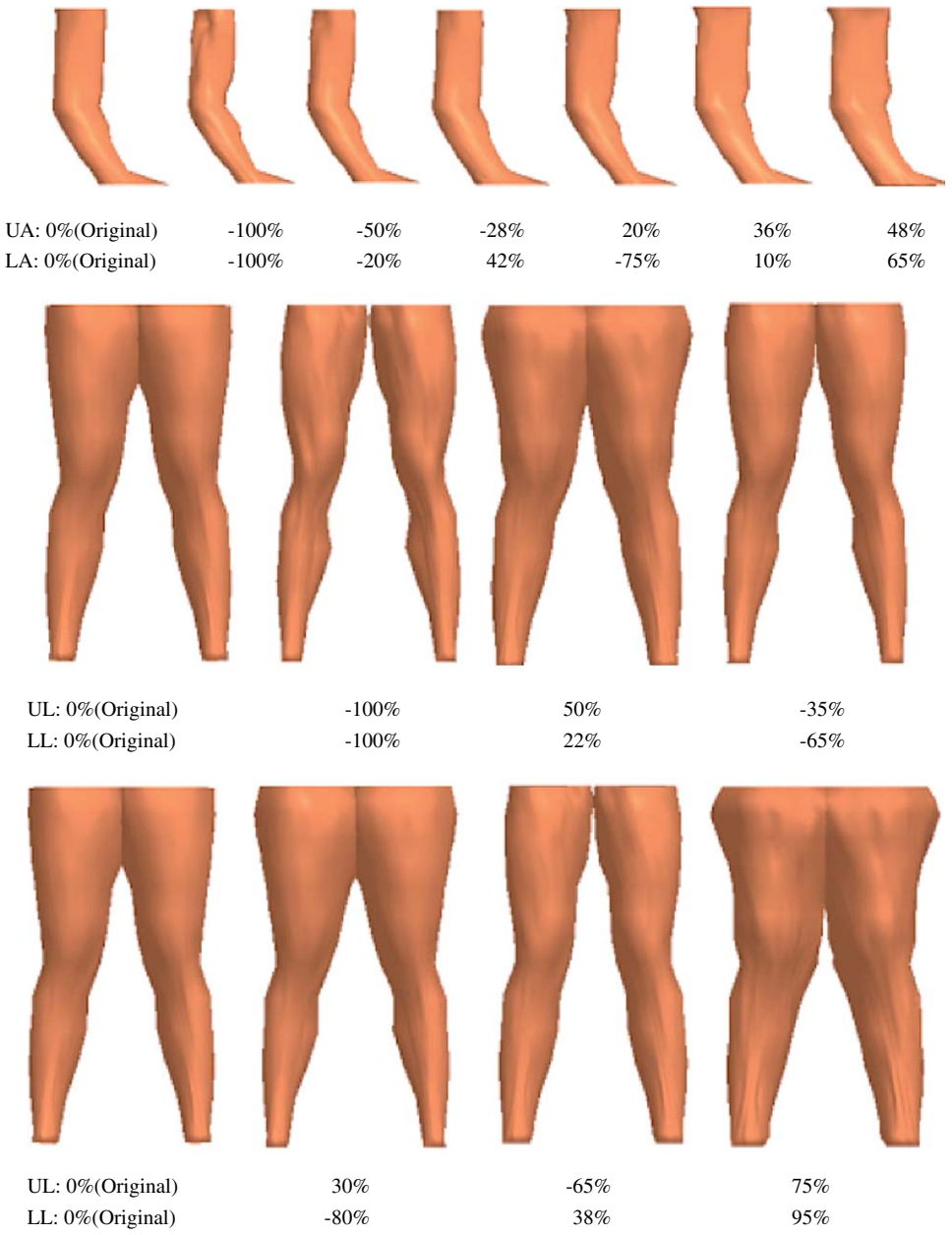

Fig. 18. Limb models of varied fat percentage values of upper and lower limbs.

Fig. 19 shows a range of fatness morphed whole body models generated from a single 3-layered generic model, given different combinations of body part fat percentages. Table 3 lists different sets of normalised body part fat percentages used to generate the whole body models in Fig. 19.

According to global body attributes (e.g. *hip-to-waist ratio*), the resulting models can be categorised into a few typical body types: *Hourglass*, *Pear*, *Apple*, etc. Meanwhile, within each category, each model has an individualised fat distribution pattern, given varied fat percentage value of different body parts. For instance, although models (c) and (h) have a globally similar *hourglass* shape, their fatness conditions on each body part are notably different. Model (h) has generally fatter upper limbs than lower limbs, and fatter lower torso than upper torso, whilst model (c) has the opposite fat distribution features (see Fig. 19 and Table 3). Meanwhile, the exact fat percentage value of each body part is also different in each model. This individual-to-individual body variation conforms to the situation of the real-world population where everyone's body is different from each other with a unique fat distribution pattern. In this sense, the parameterised shape modification approaches [10,12] that utilise only global control parameters (e.g. hip-to-waist ratio, whole body fat percentage, body weight/height) are less suitable to depict subtle body variations without referring to a large number of scanned body examples.

Different from the 2-layered (skeleton–skin) template model employed in most of the current example-based approaches [10–12] where the global parameter-to-geometry correlations are established over a large base of example bodies (250 in [10], 100 in [12]), each single 3-layered (skeleton–fat tissue–skin) template adopted in our approach can generate an unlimited number of new body shapes (given different combinations of body part fat percentages and other shape parameters) on its own without resorting to any existing examples as prerequisite. Meanwhile,

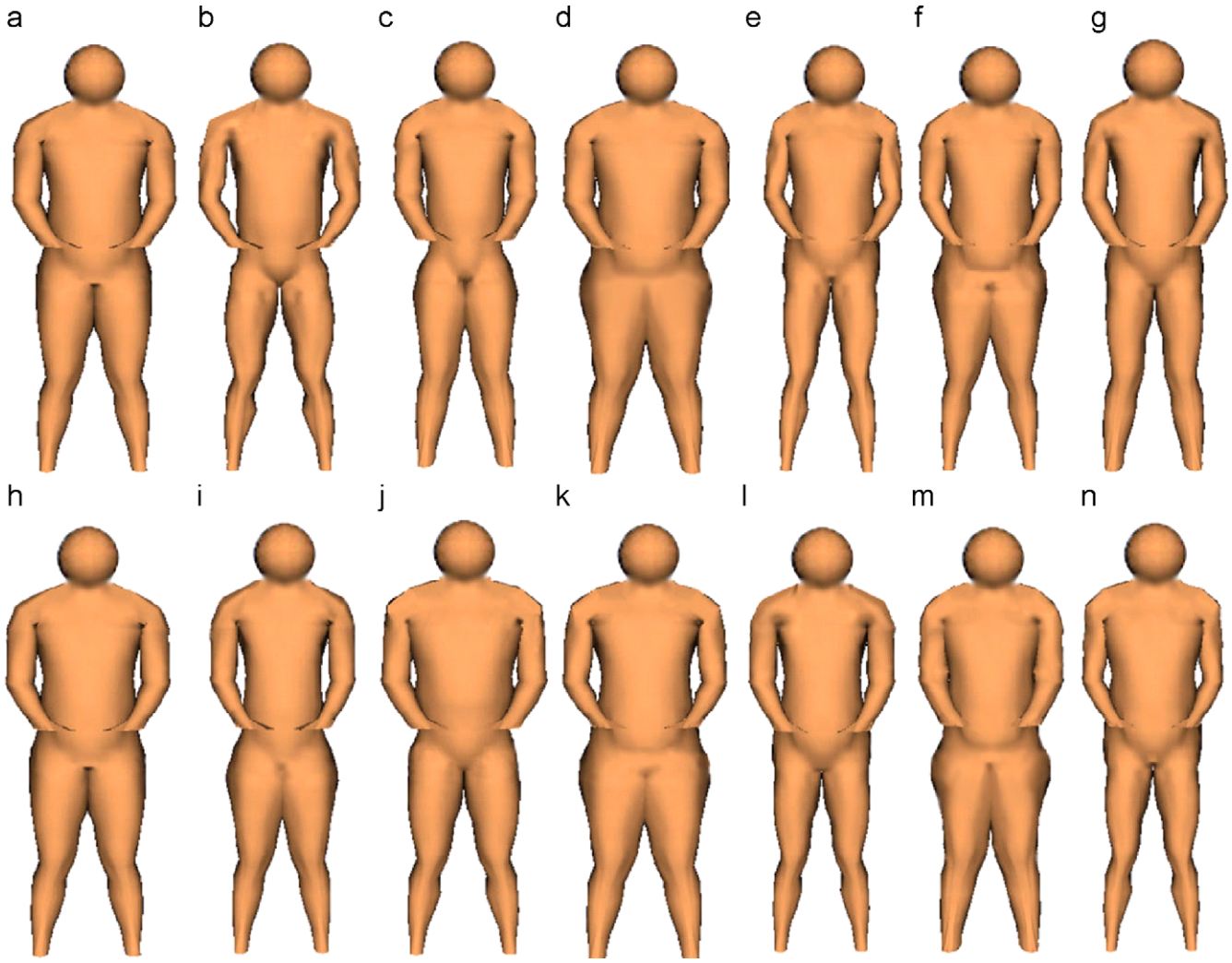

Fig. 19. Whole body models with varied fat percentage value on each individual body part. Example (a) represents the original model. Here, each model has an equal body size/proportion but different body fat distribution.

Table 3
Body part fat percentages used to generate whole body models shown in Fig. 18.

Subject	Upper arm (%)	Lower arm (%)	Upper leg (%)	Lower leg (%)	Upper torso (%)	Lower torso (%)	Shoulder (%)
(a)	0	0	0	0	0	0	0
(b)	−100	−100	−100	−100	−100	−100	−100
(c)	34	56	29	68	−14	−72	28
(d)	16	25	62	54	40	15	20
(e)	−79	−90	−84	−93	37	16	25
(f)	20	−75	56	−48	20	18	12
(g)	−53	47	−61	84	−72	5	−26
(h)	12	−16	49	7	−91	−23	−11
(i)	−20	32	−37	−60	55	−31	46
(j)	−32	−60	52	18	−50	11	30
(k)	21	12	−72	−45	−67	14	−56
(l)	53	78	75	92	73	16	41
(m)	−57	−83	−91	−76	64	17	52

each newly generated model is readily animatable and morphable in both geometric and physical senses to produce more new body shapes. Moreover, since all layered models generated from CT image processing or generic morphing share an identical mesh structure, they can be linearly interpolated or input into current example-based methods to further enlarge the space of human body variations. In addition, this technique could potentially be utilised to approximate the body-fattening process of a human subject and estimate his (her) rough appearance when (s)he gains or loses weight. Here, the body fat grows or loses based on the fat

distribution pattern of the original body. In the future, more physical layers such as a muscle layer and its physical morphing can be introduced into the current 3-layered model to generate a greater variety of human bodies, which can be classified by basic somatotypes—ectomorphic, mesomorphic, and endomorphic [36] according to the ratio of the body fat and muscle composition.

9. Implementation and user experiences

Our prototype modelling and animation interface VHS is implemented by Microsoft Visual C++, MATLAB, OpenGL, and VRML. It has been tested on a variety of input devices: electric whiteboard, Tablet PC, as well as a standard mouse.

VHS has been tested by 10 different users (5 design undergraduates, 1 engineering postgraduate, 1 social science postgraduate, 1 artist, 1 animator, and 1 12-year-old boy) to assess its usability and functionalities through performance tests, sketching observation, and user interviews. After a short tutorial, each user was requested to create 3D human bodies and animation in the following two scenarios:

Scenario 1—Users sketch-out a 3-frame stick figure (SF) jumping animation on a Tablet PC. The four steps to be followed to obtain the resulting animation are: *key framing*, *depth gesture indication*, *pose reconstruction*, and *graphical motion definition*.

Scenario 2—Users sketch-out a 3-frame full figure (FF) Chinese Kungfu animation on a Tablet PC. The five steps to be followed to obtain the resulting animation are *key framing*, *fleshing-out*, *depth gesture indication*, *pose reconstruction*, and *graphical motion definition*.

The 3D key poses in each animation (SF–jumping, FF–Kungfu) were pre-defined and shown to users, so that they could depict them through 2D sketching to achieve similar results. The evaluator timed and observed every individual task during the creation process.

In both tests, users' creation times varied from 3.75 min (SF by the animator) and 4.3 min (FF by the artist) to 8.5 and 9.75 min (SF/FF by the engineering student who tended to draw particularly precisely). The average creation time (SF: 6.27 min, FF: 6.75 min) is in considerable contrast with commercial packages, which usually require dozens of minutes and several hours, respectively for an animator to create similar articulated and full figure animation from scratch. In terms of the speed and the animation quality, the top 3 users were the animator, the artist, and one of the design students. This indicates that the sketching/animating routine in VHS is somewhat similar to their real practice. Thus, they were able to tune into it rapidly and effectively. It was also delightful to see that the young boy (only 12 years old) could sketch-out a 3D stick figure and a full figure animation enjoyably in just 6.5 and 8.34 min. This demonstrates how easy and intuitive VHS is to enable novices (with minimum skill) to create their own animations by sketching.

From the stick figure to the full figure section, users' average time on each individual task was noticeably reduced: *key framing* (2.54→2.51 min), *depth gesture indication* (1.50→1.05 min), *3D reconstruction* (0.93→0.59 min), and *motion* definition (1.30→0.67 min). This suggests the learnability of VHS, which allows users to incrementally master it through previous usages. In the full figure section, users spend averagely only 1.93 min on "fleshing-out" (even quicker than paper-based drawing in our initial sketching experiments) to create various 3D human bodies. Fig. 14 (top) shows the sketches and various human bodies created by users during the test. These sketch-generated virtual characters have been integrated into two group animations, shown in Fig. 14 (bottom). More details on our user tests and studies, as well as our user-centred and scenario-based design approaches have been presented in [37].

10. Limitations and future work

This paper presents a sketch-based human body modelling approach, which is able to produce plausible human body models through a sketching interface. As common, any method has its own pros and cons. Our approach and the current VHS have some limitations, which need to be addressed in the future.

First, our "On-Line Stroke Processing Method" needs to be improved to handle more complicated figure poses (e.g. lying, arm crossed), views (e.g. top, back views), where the system may group sketch strokes into wrong body parts and thus produce unexpected modelling results. This can be partially solved by utilising our "Stick Figure→Fleshing-out→Skin Mapping" pipeline, where the user can choose to flesh-out body contours in a relatively "easy" figure posture/view (with less overlying area) to create the initial body surface. Then, surface mapping is performed to obtain the models in relatively "difficult" poses. Meanwhile, techniques need to be investigated to handle "badly" sketched figures and self-intersections of the reconstructed mesh for folded postures. More rendering forms such as shading and shadow need be included to depict subtle surface features. In addition, sketch-based modelling of human heads/hands/feet and clothes needs to be enabled to deliver more sophisticated character models.

Second, our current sketch-based modelling approach achieves limited realism, since modelling artefacts (such as slightly jaggy/bumpy surfaces) appear on reconstructed 3D body models sometimes. This may be caused by several issues: (1) our simplified template model with only 13 basic joints, sparse body cross-sections and casting rays; (2) simplified linear interpolation utilised for surface matching during a 2D–3D modelling process; (3) lack of other internal layers such as the muscle layer integrated in the current multi-layered template mechanism. In the future, we plan to refine our current generic model by increasing the number of body joints, cross-sections, and casting rays for more accurate skin deformation, fat distribution digitisation, and body feature extraction. Since body auto-beautification should preferably include a surface smoothing process, we propose to perform a curve fitting process to fit the sparse sketch feature points onto smooth parametric contour curves before surface matching to ensure the smoothness of the resulting surface. Meanwhile, we plan to introduce more physical layers (such as the muscle layer) into our current 3-layered template model to achieve more realistic modelling results (discussed below).

Third, since a simple version of "Skeleton-Driven Skin Deformation" technique [35] is utilised for skin mesh deformation in our current approach, the range of poses that deliver plausible skin deformation effects is limited because of the undesirable deformation artefacts around the area of complicated joints (shoulder/pelvis) when bending and twisting. Meanwhile, the quality of skin surfaces from the current skin deformation method is somehow plausible but not flawless compared with the expected quality. We are going to utilise skeletal skin deformation functions in 3DS MAX through a commercial plug-in [38] to the current system for accomplishing fast and realistic skin deformation effects. Moreover, how to improve the quality of skin deformation is still a well known and challenging problem for the research community.

Next, although a simplified 3-layered (skeleton–fat tissue––skin) template is adopted in our current approach, the actual human body composition is fairly complex comprising various physical layers including skeleton, inner volume, fat tissue,

muscle, skin, etc. Meanwhile, the distributions and thickness of different layers vary over different parts of the body. According to the size/proportion of the body frame and the prominence of basic tissue types (digestive, muscular, nervous tissues), human bodies can also be classified by somatotypes—ectomorphic (preponderance of body fat), mesomorphic (preponderance of musculature), and endomorphic (lack of fat and muscle tissues) [36]. Therefore, the consideration of a muscle layer (as a substantial part of the body), the ratio of body fat and muscle composition, and morphing of both fat and muscle layers is important for generating a wider range of human bodies with physical realism and diversity. In the future, we propose to introduce a muscle layer to form a 4-layered generic model, to investigate the means for muscle distribution assessment, and to devise a combined mechanism for both fatness and muscle morphing. This 4-layered model will also be able to support volumetric simulation [39,40], which is an alternative way of creating high-quality surface deformation. This will also enrich the human body shapes with a range of musculature variations in chest muscles, abdominal muscles, deltoid muscles, calf muscles, etc.

Finally, we need to expand our generic template database and establish a template matching/recalling scheme to enable sketch-based modelling of a population of human bodies (i.e. males, females, children, and elderly people). Although only one template model is employed in the current system, our generic model acquisition technique can be easily replicated on the CT cross-section images generated from whole body CT scanning equipment [41] and join with our template morphing scheme, to create a population of layered generic models of males, females, children, and elderly people to expand the generic template database. Since our "Creative Model-based Method" is generic to be applied to any type of template model, a template matching/recalling scheme can be established to "recall" any suitable template (e.g. male, female, etc.) from the template database according to the features of a sketched figure, to interpret its body size and shape, and then to fit the 3D template into the 2D drawing through geometric and physical morphing. In this sense, the future version of our approach can support sketch-based modelling of a wide range of human population (i.e. females, children, etc.) once an expanded generic template database and a template matching/recalling scheme are achieved.

Although the current comparison between VHS and commercial systems shows a better performance of VHS in terms of a shorter learning time, this indicator is affected by system complexity and functionality as well. Typically, commercial systems have much more functionalities and more complicated interfaces, which may require more time for users to learn how to use the systems. A sketch-based interface aims to reduce the learning overhead as well as to provide good/intuitive functionalities for a system. However, the increased functionalities in even a sketch-based system may inevitably require more learning time, for example, the increased time for users to learn more drawing gestures. Our system has relatively limited functions currently. When it becomes more functional, it may require more learning time accordingly.

11. Conclusion

Human body modelling is a recognised challenge and a labour-intensive task, which has been, until now, confined to the domain of professionals. In this paper, we have presented a new method and a novel interface VHS, which draws on the existing drawing skills of ordinary people to create 3D virtual human models quickly and enjoyably. The highlights of this work include the support of a natural figure drawing input/process, a "Creative Model-based Method" performing 2D–3D human body reconstruction via multi-layered generic models, a 3-layered generic model for undertaking both geometric and physical morphing, and a sketch-based global/local surface modification approach.

Featured as a fast, easy, and low-cost tool, VHS has potentials to benefit various users. Non-professionals can use it as an entertaining tool to sketch-out imaginative 3D characters and animate them in a virtual world easily and enjoyably. 2D artists can visualise their initial character design and storyboards in 3D and modify them in early design stages, through sketching as an intuitive and familiar medium [21]. Professional modellers/animators can utilise VHS as a rapid prototyping tool to generate quick and intermediate 3D human body models and motions, which can be exported into commercial tools for further refinement. In addition, our multi-layered template acquisition and morphing scheme can be utilised independently to generate various new human body shapes for common applications through direct manipulation of body parameters.

Acknowledgement

The authors would like to thank the anonymous referees for their valuable and helpful comments for improving the quality of this paper. This work was funded by the Brunel Innovation and Enterprise Fund (BRIEF) and the School of Engineering and Design of the Brunel University, UK. The authors would like to thank professor Xiao Yi and her students at Beijing Jiaotong University, and Professor Jun Peng and his students at Tianjin Academy of Fine Arts for heir helps in evaluation.

Appendix

A.1. Stroke identification

For stroke identification, it is presumed that a bone is more likely to be rendered when it has a closer orientation and/or

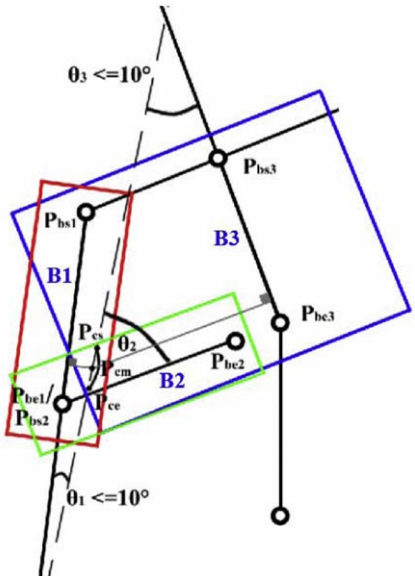

Fig. A.1. Stroke identification for a curve stroke locating in the bounding boxes of multiple bones. First, compute the in-between angle θ_1, θ_2, and θ_3 of the stroke and the corresponding bones (B1: left upper arm, B2: left lower arm, and B3: upper torso) in an *orientation check*. Since θ_1 and θ_3 are $\leqslant\delta$, B1 and B3 are passed to the *distance check*. Since B1 has a smaller distance to the stroke than B3, the stroke is finally identified as a rendering stroke for B1 (left upper arm).

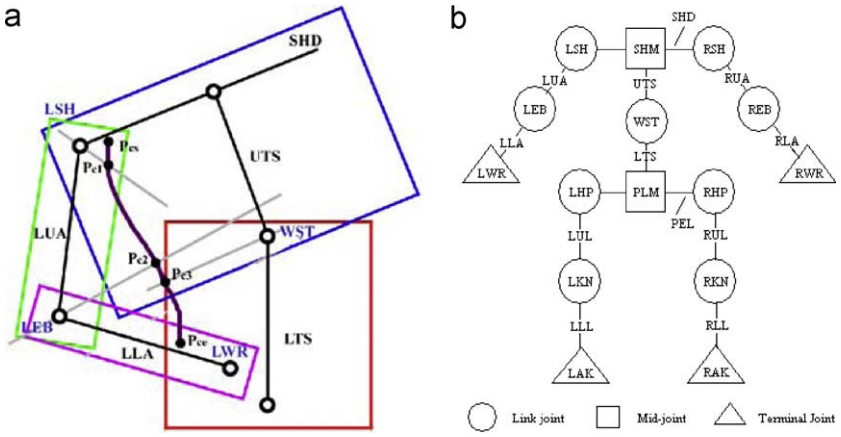

Fig. A.2. (a) Stroke segmentation for a long stroke spanning multiple bone areas. First, find different groups of influential bones (UTS/LTS, UTS/LUA/LLA, LUA/LLA) according to different pairs of B_s and B_e (UTS-LTS, UTS-LLA, LUA-LLA), which locate the start and end points of the given stroke. Then, segment the stroke with the joint angles midlines (WST, WST/LSH, LEB) in-between the neighbouring bones within each pair of B_s and B_e, and compute the corresponding A_{avg} and D_{avg} value. Finally, the stroke is identified as spanning UTS and LTS after the orientation and distance check. (b) Abstracted human body structure labelled by abbreviations of bones and joints.

distance to a given stroke than other candidate bones. Here, the orientation similarity is given a higher priority since most human body parts have a cylindrical structure where a body contour roughly follows the direction of the underlying bone. The stroke identification process here comprises an *orientation check* followed by a *distance check*. In the *orientation check*, all candidate bones that have a small enough in-between angle δ ($\delta = 10^\circ$) with the curve stroke are kept and passed to a *distance check*. Here, δ value is heuristically defined and can be adjusted according to needs. In the *distance check*, the bone that has a minimum distance to the curve stroke compared with the remaining bones is identified as the bone rendered by the given stroke. Here, if there is no bone whose $\theta \leqslant \delta$, the bone that has a minimum θ value compared with others is taken as the identified bone. Fig. A.1 illustrates this curve identification process.

In the *orientation check*, given the start point $P_{cs}(X_{cs},Y_{cs})$ and end point $P_{ce}(X_{ce},Y_{ce})$ of a curve, its orientation can be approximated as: $C = (X_{ce}-X_{cs})i+(Y_{ce}-Y_{cs})j$. Given the start point $P_{bs}(X_{bs},Y_{bs})$ and end point $P_{be}(X_{be},Y_{be})$ of a bone, its orientation can be approximated as: $B = (X_{be}-X_{bs})i+(Y_{be}-Y_{bs})j$. Then, the in-between angle θ of curve and bone vectors[1] is computed through a scalar product equation:

$$\theta = a\cos\left(\frac{(CB)}{|C||B|}\right) = a\cos\left(\frac{(X_{ce}-X_{cs})(X_{be}-X_{bs})+(Y_{ce}-Y_{cs})(Y_{be}-Y_{bs})}{\sqrt{(X_{ce}-X_{cs})^2+(Y_{ce}-Y_{cs})^2}\times\sqrt{(X_{be}-X_{bs})^2+(Y_{be}-Y_{bs})^2}}\right) \quad (A.1)$$

In a *distance check*, an approximate stroke average point $P_{cm}(X_{cm} = (X_{cs}+X_{ce})/2,\ Y_{cm} = (Y_{cs}+Y_{ce})/2)$ is used to calculate the distance between a curve stroke and a candidate bone.

A.2. Stroke segmentation

When a long stroke spans more than one bone-bounding area, it is segmented by the mid-lines of the joint angles that are in-between pairs of neighbouring bones spanned by the curve stroke.

[1] Here, when θ is an obtuse angle, it is converted to its corresponding acute angle considering the variations of the corresponding curve/bone start and end points.

As shown in Fig. A.2a, stroke segmentation starts by searching the locating bone(s) B_s and B_e of the start point P_{cs} and end point P_{ce} of a curve stroke. Here, given B_s and B_e, the influential bones spanned by a given stroke and the joints on the segmentation mid-lines can be determined based on a fixed human body topology (see Fig. A.2b). If the start point P_{cs} (end point P_{ce}) is found inside more than one bone-bounding box, different possible pairs of B_s and B_e are listed. For each candidate pair, the stroke is segmented into separate pieces by its specific combination of joint mid-lines. For each curve segment, its in-between angle θ_n and distance D_n with its associated bone are calculated and saved. Then, an average angle A_{avg} ($A_{avg} = (\sum_{n=1}^{m}\theta_n)/m$) and distance D_{avg} ($D_{avg} = (\sum_{n=1}^{m}D_n)/m$) for each candidate pair is computed, where m is equal to the number of segments on the curve. Next, the A_{avg} value of each candidate pair is compared with δ ($\delta = 10^\circ$). The ones who's $A_{avg} \leqslant \delta$ are saved and passed to a distance check. As before (see (A.1)), the candidate pair that has a minimum D_{avg} value is taken. Next, each segmented curve is indexed and saved into its corresponding bone determined by the identified pair.

A.3. Hermit spline interpolation for computing the scaling factors of ROI points

As shown in Fig. A.3, given the previously recorded N^l and N^r value and the S_s value (of the silhouette column point) for each layer, the ray scaling factors ($S_{s,i}$) of other influential points on this layer are computed through a Hermit spline interpolation. As illustrated, P_{k+1} represents a silhouette column point with a ray scaling factor S_s. P_k and P_{k+2} represent the leftmost and rightmost ROI points on the given cross-section layer. The ray scaling factors of ROI points in-between point P_k and P_{k+1}, and point P_{k+1} and P_{k+2} are computed through a Hermit blending function:

$$P(u) = \mathrm{p}_k(2u^3-3u^2+1)+\mathrm{p}_k+1(-2u^3+3u^2) + \mathrm{D}_{\mathrm{p}_k}(u^3-2u^2+u)+\mathrm{D}_{\mathrm{p}_k}+1(u^3-u^2), \quad 0\leqslant u\leqslant 1 \quad (A.2)$$

The corresponding point p_k and Dp_k value (tangent vector) has been labelled on Fig. A.3. Here, $t = 0.5$, which is determined by adjusting t value and visually evaluating the resulting local surface deformation. Ideally, the t value should be adjusted by

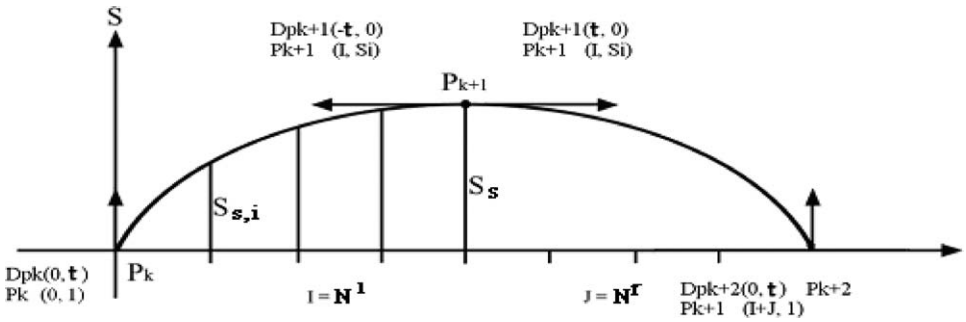

Fig. A.3. Calculating the ray scaling factor for each ROI point through a Hermit spline interpolation.

users' interactive control (such as mouse dragging or dropping). This function is to be implemented in the future system.

References

[1] Wilhelms J, Van Gelder A. Anatomically based modeling, In: Proceedings of SIGGRAPH '97, ACM SIGGRAPH, 1997. p. 173–80.
[2] Turner R, Gobbetti E. Interactive construction and animation of layered elastically deformable characters. Computer Graphics Forum 1998;17(2):135–52.
[3] Choi JJ. MAYA character animation. 2nd ed. London, San Francisco, CA: SYBEX; 2004.
[4] Magnenat-Thalmann N, Thalmann D. The direction of synthetic actors in the film Rendez-vous à Montréal. IEEE Computer Graphics and Applications 1987;7(12):9–19.
[5] Fua P. Human modeling from video sequence. Geometric Info Magazine 1999;13(7):63–5.
[6] Hilton A, Beresford D, Gentils T, Smith R, Sun W. Virtual people: capturing human models to populate virtual worlds. In: Proceedings of Computer Animation. IEEE Press; 1999. p. 174–85.
[7] Lee W, Gu J, Magnenat-Thalmann N. Generating animatable 3D virtual humans from photographs. Computer Graphics Forum 2000;19(3):1–10.
[8] Cordier F, Magnenat-Thalmann N. Real-time animation of dress virtual humans. Computer Graphics Forum 2002;21(3):327–36.
[9] Sloan PP, Rose C, Colen M. Shape by example. Symposium on Interactive 3D Graphics 2001. p. 135–43.
[10] Allen B, Curless B, Popovis Z. The space of all body shapes: reconstruction and parameterization from range scans. In: Proceedings of SIGGRAPH '03, ACM SIGGRAPH, 2003. p. 587–94.
[11] Anguelov D, Srinivasan P, Koller D, Thrun S, Rodgers J. SCAPE: shape completion and animation of people, In Proceedings of SIGGRAPH '05, ACM SIGGRAPH, 2005, p. 408–16.
[12] Seo H, Magnenat-Thalmann N. An example-based approach to human body manipulation. Graphical Models 2004;66(1):1–23.
[13] Igarashi T, Matsuoka S, Tanaka H. Teddy: a sketching interface for 3D freeform design. In: Proceedings of SIGGRAPH '99, ACM SIGGRAPH, 1999. p. 409–16.
[14] Karpenko O, Hughes JF, Raskar R. Free-form sketching with variational implicit surfaces. Proceedings of Eurographics 2002;21(3):585–94.
[15] Alexe A, Gaildrat V, Barthe L. Modelling from sketches using spherical implicit functions. In: Proceedings of third international conference on computer graphics, Virtual reality, visualisation and interaction in Africa, 2004. p. 25–34.
[16] Turquin E, Wither J, Boissieux L, Cani M-P, Hughes JF. A sketch-based interface for clothing virtual characters. IEEE Computer Graphics and Applications 2007;27(1):72–81.
[17] Karpenko OA, Hughes JF. SmoothSketch: 3D free-from shapes from complex sketches. ACM Transactions of Graphics 2006;25(3):589–98.
[18] Tiner R. Figure drawing without a model. Glasgow: David & Charles Plc.; 1992.
[19] Li W. Figure drawing: basic pose and construction, FARP 〈http://elfwood.lysator.liu.se/farp/figure/williamlibodyconstruction.html〉, 2008.
[20] Greg A. Basic figure drawing techniques. Cincinnati, OH: North Light Books; 1994.
[21] Mao C, Qin SF, Wright DK. Sketching-out virtual humans: from 2D storyboarding to immediate 3D character animation. In: Proceedings of ACM SIGCHI international conference on advances in computer entertainment technology. Hollywood, Los Angeles, 2006.
[22] Mao C, Qin SF, Wright DK. A sketch-based gesture interface for rough 3D stick figure animation. In: Proceedings of Eurographics workshop on sketch based interfaces and modeling, 2005. p. 175–83.
[23] Magnenat-Thalmann N, Seo H, Cordier F. Automatic modeling of virtual humans and body clothing. In: Proceedings of 3-D digital imaging and modeling. IEEE Computer Society Press; 2003. p. 2–10.
[24] Seo H, Yahia-Cherif L, Goto T, Magnenat-Thalmann N. GENESIS: generation of e_population based on statistical information. In: Proceedings of computer animation '02. IEEE Computer Society Press; 2002. p. 81–5.
[25] Tai CL, Zhang HX, Fong J C-K. Prototype modeling from sketched silhouettes based on convolution surfaces. Computer Graphics Forum 2004;23(1):71–83.
[26] Schmidt R, Wyvill B, Sousa MC, Jorge JA. ShapeShop: sketch-based solid modeling with BlobTrees. In: Proceedings of Eurographics workshop on sketch-based interfaces and modeling. 2005. p. 53–62.
[27] Thalmann D, Shen JH, Chauvineau E. Fast realistic human body deformations for animation and VR applications. In: Proceedings of Computer Graphics. International IEEE Computer Society Press; 1996. p. 166–74.
[28] Nealen A, Sorkine O, Alexa M, Cohen-Or D. A sketch-based interface for detail-preserving mesh editing. ACM Transaction on Graphics (TOG) 2005;24(3):1142–7.
[29] Davis J, Agrawala M, Chuang E, Popović Z, Salesin D. A sketching interface for articulated figure animation. In: Proceedings of Eurographics/SIGGRAPH symposium on computer animation, 2003. p. 320–28.
[30] Hoshino J, Hoshino Y. Intelligent storyboard for prototyping animation. In: Proceedings of IEEE international conference on multimedia and expo, 2001, Conference CD-ROM FAI.03.
[31] Hecker R, Perlin K. Controlling 3D objects by sketching 2D views. SPIE—Sensor Fusion 1992;1828:46–8.
[32] Chaudhuri P, Kalra P, Banerjee S. A system for view-dependent animation. Computer Graphics Forum 2004;23(3):411–20.
[33] Lipson H, Shpitalni M. Correlation-based reconstruction of a 3D object from a single freehand sketch. In: Proceedings of AAAI Spring symposium series—sketch understanding, 2002.
[34] National Library of Medicine. The Virtual Human Project 〈http://www.nlm.nih.gov/research/visible/visible_human.html〉, 2008.
[35] Weber J. Run-time skin deformation. Intel Architecture Labs 〈http://www.intel.com/ial/3dsoftware/index.htm〉, 2000.
[36] Wikipedia. Somototype 〈http://en.wikipedia.org/wiki/mesomorphic〉, 2008.
[37] Mao C, Qin SF, Wright DK, Peng J. Applying scenarios in user-centred design to develop a sketching interface for human modelling and animation. In: Proceedings of Eurographics workshop on sketch based interfaces and modeling, 2006. p. 147–56.
[38] Bone Pro 3. 〈http://www.3d-shop.net/Details.cfm?ProductID=108〉, 2008.
[39] Popa T, Julius D, Sheffer A, Material-aware mesh deformations. In: Proceedings of the IEEE international conference on shape modeling and applications, 2006 (SMI'06).
[40] Bro-Nielsen M, Cotin S. Real-time volumetric deformable models for surgery simulation using finite elements and condensation. Computer Graphics Forum 1996;15(3):57–66.
[41] Information on whole body scanning 〈http://www.epa.nsw.gov.au/radiation/ctbodyscans.htm〉, 2008.